

Article

Not peer-reviewed version

---

# Enumeration of N-dimensional Hypercube, Icosahedral, Rubik's Cube Dice, Colorings and Encryptions Based on Their Symmetries

---

[Krishnan Balasubramanian](#) \*

Posted Date: 24 July 2024

doi: 10.20944/preprints2024071853.v1

Keywords: Monte Carlo Enumeration of n-dimensional dice; icosahedral and hypercubic symmetries; buckminsterfullerene; mesoporous and zeolite materials; isochiral polyhedra; cryptography



Preprints.org is a free multidiscipline platform providing preprint service that is dedicated to making early versions of research outputs permanently available and citable. Preprints posted at Preprints.org appear in Web of Science, Crossref, Google Scholar, Scilit, Europe PMC.

Copyright: This is an open access article distributed under the Creative Commons Attribution License which permits unrestricted use, distribution, and reproduction in any medium, provided the original work is properly cited.

## Article

# Enumeration of n-Dimensional Hypercube, Icosahedral, Rubik's Cube Dice, Colorings and Encryptions Based on Their Symmetries

Krishnan Balasubramanian

School of Molecular Sciences, Arizona State University, Tempe, AZ 85287-1604, USA; kbalu@asu.edu

**Abstract:** The whimsical Las Vegas/Monte Carlo cubic dice are generalized to construct the combinatorial problem of enumerating all n-dimensional hypercube dice, and dice of other shapes that exhibit cubic, icosahedral and higher symmetries. By utilizing powerful generating function techniques for various irreducible representations, we derive the combinatorial enumerations of all possible dice in n-dimensional space with hyperoctahedral symmetries. Likewise a number of shapes that exhibit icosahedral symmetries such as a truncated dodecahedron and a truncated icosahedron are considered for the combinatorial problem of dice enumerations with the corresponding shapes. We consider several dice with cubic symmetries such as truncated octahedron, dodecahedron and Rubik's cube shapes. It is shown that all enumerated dice are chiral and we provide the counts of chiral pairs of dice in the n-dimension space. During the combinatorial enumeration, it was discovered that two different shapes of dice exist with the same chiral pair count culminating into the novel concept of isochiral polyhedra. The combinatorial problem of dice enumeration is generalized to multi-coloring partitions. Applications to chirality in n-dimension, molecular clusters, zeolites, mesoporous materials, cryptography and biology are also pointed out. Applications to nonlinear n-dimensional hypercube and other dicey encryptions are exemplified with romantic, clandestine messages; "I love U" and "V Elope at 2".

**Keywords:** Monte Carlo Enumeration of n-dimensional dice; icosahedral and hypercubic symmetries; buckminsterfullerene; mesoporous and zeolite materials; isochiral polyhedra; cryptography

## 1. Introduction

The Monte Carlo/Las Vegas dice are special cases of face colorings of a cube with 6 different numbers/colors under cubic rotational symmetry action stipulating that the sum of numbers on the opposite sides of the cube add to 7. There are exactly 30 possible dice or 15 chiral pairs without any such constraints, and yet only one die is chosen for gambling. Even though a chiral pair of dice exist with the stipulation that the sum of opposite sides shall be 7, only the right-handed die is the favorite of the Las Vegas world of gambling. Yet stimulated by several applications, there are scholarly reasons to consider all possible dice enumerations not only in the 3D-space but also the dice and coloring enumerations in n-dimensions. Furthermore consideration of other shapes of dice such as a truncated octahedron, truncated icosahedron and so forth could have several applications in chemistry, material science, and biology including molecular structures arising from face cappings of such three-dimensional molecular structures to genetic regulatory networks [1–33]. The generalization of these combinatorial enumeration problems to n-dimensional hypercubes, polycubes, polytopes, molecular bodies, and databases [1–33] and the related combinatorics of hyperoctahedral or wreath product groups can have profound ramifications in several fields [34–58]. A phenomenal exemplification of such applications is to the cynosure of wreath product objects namely, the celebrated Rubik's cube, which in general symmetry terms, is a quintessential element of dynamic symmetry and coloring under the wreath product symmetry action.

The n-dimensional hypercubes are ubiquitous in varied fields such as artificial intelligence, pattern recognition, visual image processing, electrical circuit theory, information science including

Boolean logic, where the  $2^n$  possible Boolean strings become the vertices of an  $n$ -dimensional hypercube [34–58]. Furthermore hypercubes find applications in biology, chemistry, isomerization reactions, finite automata, enumeration of isomers, genetics, computer graphics, chirality, protein-protein interactions, intrinsically disordered proteins and their moonlighting functions, computational psychiatry, partitioning of big data, and parallel computing [34–58]. The recursive nature of symmetries of hypercubes can be molded into hyperoctahedral wreath products [1]. These recursive symmetries find numerous applications in isomerization reactions, enumerative combinatorics, nuclear spin statistics, water clusters, non-rigid molecules, proteomics, and spontaneous generation of chirality, a phenomenon made possible by chiral reaction pathways in isomerization graphs [1,34–58]. The  $nd$ -boolean hypercubes find their ways into novel representations of time measures, periodic table of elements, quantum similarity measures, and so forth [4–9], biochemical and multi-dimensional imaging [11], big data, Quantitative Shape-Activity Relations (QShAR), and so forth [12–15].

Combinatorial enumeration of face colorings of  $n$ -dimensional hypercubes has a direct bearing to the subject matter of this study, although the vertex-coloring of  $n$ -dimensional hypercubes has been the subject matter of numerous studies over the years. Pólya [22,23] alluded to the errors propagated in earlier works on the enumeration of colorings of vertices  $nD$ -hypercubes. The topic has attracted numerous researchers for decades culminating into a plethora of publications owing to their interest in multiple fields [20–58]. In the present study we apply the face colorings of hypercubes not only to the problem of dice enumerations in  $n$ -dimension but also point out several other applications with different color partitions. Furthermore several chemical and spectroscopic applications require generalized combinatorial/group theory enumeration techniques that include *all the irreducible representations of the groups* whereas Pólya's theorem reduces to a special case, namely the one for the totally symmetric representation. In the present study, we consider the enumeration of dice and face colorings of not only objects of cubic symmetries but also icosahedral symmetries such as a truncated icosahedron and so on which find applications in the representation of the celebrated buckminsterfullerene. Consequently, these techniques would find natural applications to mesoporous materials, zeolites and large highly symmetric fullerene cages including the golden fullerenes and nanospheres. Furthermore, the enumeration of  $n$ -dimensional dice and colorings could have profound implications in cryptography in encrypting and decrypting messages through face-labeled packets of  $nd$ -hypercubes and icosahedral structures.

## 2. Combinatorial and Group Theoretical Techniques

The symmetry group of an  $nD$ -hypercube is an hyperoctahedral group which can be cast into the wreath product form  $S_n[S_2]$  where  $S_n$  is the full permutation group of  $n$  objects with  $n!$  permutations. Consequently, the cardinality of the  $nD$ -hypercube group is  $2^n \times n!$ . For example, the asymmetry group of a 10-rcube contains  $2^{10} \times 10!$  permutations spanning 481 conjugacy classes, and 481 irreducible representations. Moreover, there are 10 hyperplanes for a 10-cube, and hence enumerating colorings of different hyperplanes of an  $nD$ -hypercube for all irreducible representations can be combinatorial a complex and daunting problem which provides a perfect platform for artificial intelligence. Coxeter [59] has carried out ground-breaking work on the characterization of hypercubes and several other regular polytopes. An  $nD$ -hypercube contains  $(n-q)$ -hyperplanes where  $q$  goes from 0 to  $n$ . The largest value of  $q = n$  represents the vertices,  $q=n-1$  represents the edges,  $q=n-2$  represents the faces, and so on. In the present study we focus on the face colorings and their combinatorial enumerations. The induced permutation arising from the action of the symmetry group of the  $nD$ -hypercube on each of these hyperplanes require complex mathematical techniques involving polynomial generators and Möbius inversion techniques both of which have been discussed extensively in previous studies. Hence we will not repeat these details and restrict ourselves to face colorings. Moreover we consider the enumerations that involve all irreducible representations which require the cycle types of each conjugacy class, which are constructed from matrices of the conjugacy classes of wreath product groups.

Consider a 7D-hypercube or briefly denoted as a 7-cube. The geometrical structure of a t-cube is characterized by a  $7 \times 7$  configuration matrix in Coxeter's notation [59] exemplified here where the rows are  $q$  values in reverse order, ( from 7 to 1) as they represent  $(n-q)$ -hyperplanes of the  $n$ -cube.

$$\begin{pmatrix} 128 & 7 & 21 & 35 & 35 & 21 & 7 \\ 2 & 448 & 6 & 15 & 20 & 15 & 6 \\ 4 & 4 & 672 & 5 & 10 & 10 & 5 \\ 8 & 12 & 6 & 560 & 4 & 6 & 6 \\ 16 & 32 & 24 & 8 & 280 & 3 & 3 \\ 32 & 80 & 80 & 40 & 10 & 84 & 2 \\ 64 & 192 & 240 & 160 & 60 & 12 & 14 \end{pmatrix}$$

The number of  $(n-q)$ -hyperplanes for an  $n$ -hypercube is obtained as

$$N_q = \binom{n}{q} 2^q$$

In particular the number of faces for an  $n$ -cube is obtained as

$$N_{n-2} = \binom{n}{n-2} 2^{n-2} = \binom{n}{2} 2^{n-2} = n(n-1)2^{n-3}$$

When above formula is applied to the 7D-hypercube we obtain the number of faces as

$$\binom{7}{2} 2^5 = 672,$$

Which is the diagonal element of the third row in the above configuration matrix.

In order to enumerate the  $n$ -cube dice or in general face colorings of the  $n$ -cube with a color partition we consider a set  $D$  of faces of the  $n$ -cube with set  $R$  as the various colors such as blue, red, green, white and so on. A face coloring is then a map from the set  $D$  to set  $R$  and the combinatorial enumeration of face colorings is tantamount to enumerating the equivalence classes of such maps under the action of the symmetry cube of  $n$ -cube which is the wreath product  $S_n[S_2]$ . For example, the symmetry group of the 7-cube is isomorphic to the  $S_7[S_2]$  wreath product group which contains  $7! \times 2^7$  permutations. These permutations generate different orbit structures for each set of hyperplanes of the  $n$ -cube. In particular, for the faces of the  $n$ -cube the orbit length of the permutation acting on the faces is  $n(n-1)2^{n-3}$ , and hence the cycle types of the permutations and hence their cycle types would all be different from the cycle types and orbit structures of  $2^n$  vertices of the  $n$ -cube. We have previously demonstrated the Möbius inversion technique for the construction of cycle types and orbit structures for the various hyperplanes of the  $n$ -cube [1,3]. In summary, the Möbius inversion technique yields the orbit structure of every set of hyperplanes of the  $n$ -cube. The orbit structure is required in order to construct the generating functions for the colorings of the various hyperplanes of the  $n$ -cube.

We briefly discuss this with an illustration of the permutational cycle type of the  $S_7[S_2]$  group for each of the hyperplanes is obtained by using the Möbius inversion method. As a first step, the  $2 \times 7$  cycle type matrices for each of the 110 conjugacy classes of the 7D-hypercube which also represent the permutations of the cycle types of the hexeracts ( $q=1$ ) of the 7D-hypercube shown in Figure 1. The cycle index used in Pólya's technique, can be generalized for all irreducible representations of the  $n$ -cube's group. Consequently, one needs the cycle types for each conjugacy class of the  $S_n[S_2]$  group and for each of hyperplanes ( $q = 1, n$ ) of the  $n$ -cube. This requires the construction of the cycle types of  $q=1$  or hexeracts of the 7D-hypercube shown in Figure 1, for example. This is accomplished through matrix generators functions yielding the  $2 \times n$  matrices for the  $n$ -cube for all conjugacy classes. Subsequently, we invoke the Möbius generating function method is used to



enumerate all cycle types for  $q=2$  through  $n$ , as demonstrated in previous works for the 7-cube and 8-cube [1,39,40].

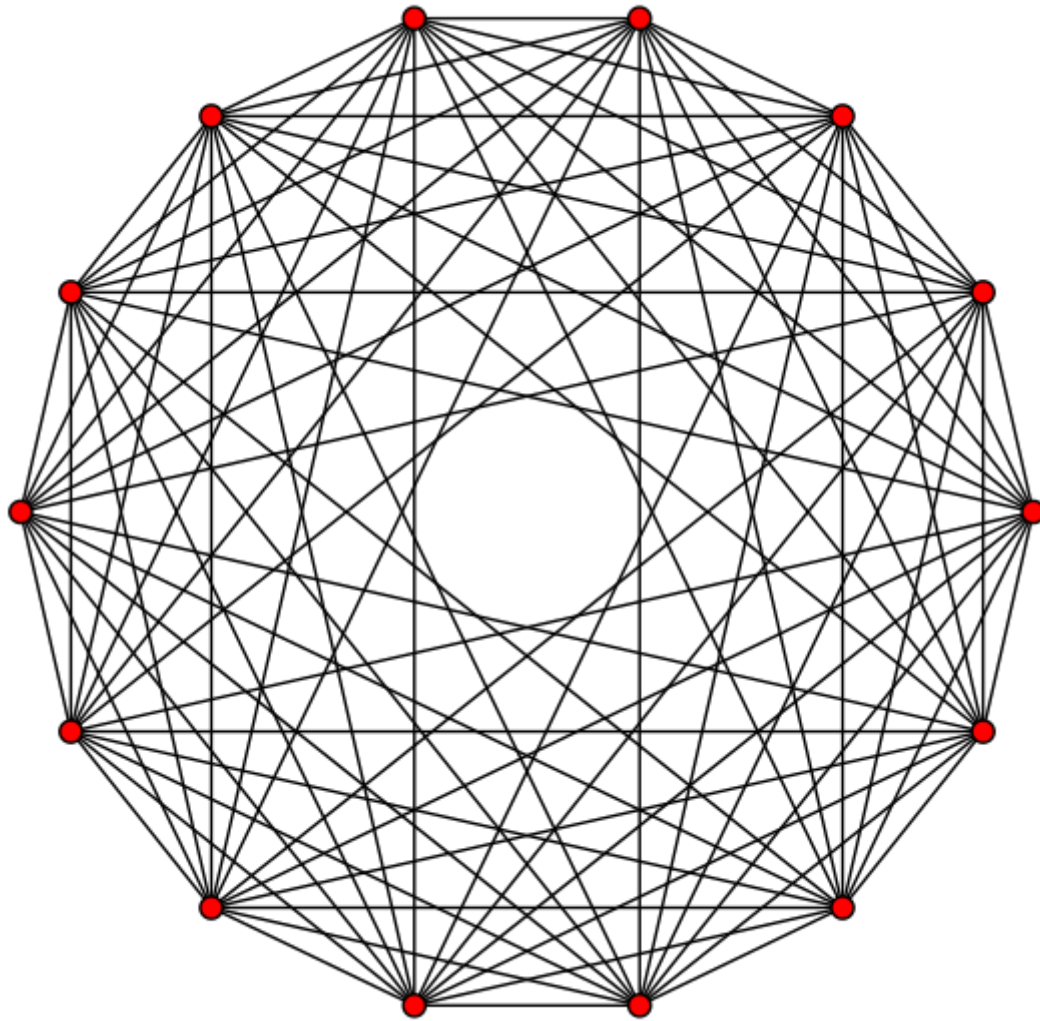


**Figure 1.** A dual representation of the 7D-hypercube in which 14 hexeracts of the 7D-hypercube are the vertices and edges representing their neighborhood connectivity. The vertices of the graph can also represent the fourteen protons of the nonrigid water heptamer,  $(\text{H}_2\text{O})_7$  in its fully nonrigid limit. (reproduced from Ref. [60]).

The character table of hyperoctahedral group containing all irreducible representations is required to construct the GCCIs of the irreducible representation  $\Gamma$  with character  $\chi$  of the group. Let the set  $D$  of the faces of the hypercube with cardinality  $l$ . In general, the GCCI for the character  $\chi$  of a group  $G'$  is defined as

$$P_{G'}^{\chi} = \frac{1}{|G'|} \sum_{g \in G'} \chi(g) s_1^{b_1} s_2^{b_2} \dots s_m^{b_m}$$

where the sum is over all permutation representations of  $g \in G'$  that generate  $b_1$  cycles of length 1,  $b_2$  cycles of length 2, ...,  $b_m$  cycles of length  $m$  upon its action on the set  $D$  of the faces of the hypercube. The generalized Pólya substitution in the GCCIs for each representation of  $S_n[S_2]$  with a multinomial expansion for coloring the faces of the hypercube with say  $r$  colors. Let  $[l]$  be an

ordered partition, also called the composition of  $l$  into  $p$  parts such that  $n_1 \geq 0, n_2 \geq 0, \dots, n_p \geq 0$ ,  $\sum_{i=1}^p n_i = l$ . A multinomial generating function in  $\lambda$ s is obtained as

$$(\lambda_1 + \lambda_2 + \dots + \lambda_p)^l = \sum_{\substack{[r] \\ n_1 n_2 \dots n_p}} \binom{l}{n_1 n_2 \dots n_p} \lambda_1^{n_1} \lambda_2^{n_2} \dots \lambda_{p-1}^{n_{p-1}} \lambda_p^{n_p}$$

where  $\binom{l}{n_1 n_2 \dots n_p}$  are multinomials given by

$$\binom{l}{n_1 n_2 \dots n_p} = \frac{l!}{n_1! n_2! \dots n_{p-1}! n_p!}$$

Let the set  $R$  which contains  $r$  different types of colors (for example, yellow, blue, green, red, white...) that can be used to color the faces of the  $n$ -cube. Let  $w_i$  be the weight of each color  $r$  in  $R$ . Consequently, the weight of a function  $f$  from  $D$  to  $R$  is defined as

$$W(f) = \prod_{i=1}^{|R|} w(f(d_i))$$

The generating function for each irreducible representation of the  $nD$ -hyperoctahedral group is obtained by the substitution as

$$GF^X(\lambda_1, \lambda_2, \dots, \lambda_p) = P_G^X \{s_k \rightarrow (\lambda_1^k + \lambda_2^k + \dots + \lambda_{p-1}^k + \lambda_p^k)\}$$

The above GFs are computed for each irreducible representation of the  $n$ -cube hyperoctahedral group. The coefficient of each term  $(\lambda_1^{n_1} \lambda_2^{n_2} \dots \lambda_p^{n_p})$  generates the number of functions in the set  $R^D$  that transform in accord with the irreducible representation  $\Gamma$  with character  $\chi$ . For the totally symmetric irreducible representation  $A_1$ , the GF reduces to the celebrated Pólya's theorem, or the enumerative GF for the number of equivalence classes of colorings. Likewise the GF for a chiral representation which would have character value of +1 for proper rotations and -1 for improper rotations would enumerate the number of chiral face colorings for a given color partition in the GF.

As these GFs become combinatorially complex with numerous terms and a large number of irreducible representations in the  $n$ -cube, computations become quite intensive. Consequently, we have automated the iterative process with Fortran '95 codes that compute the cycle types for all hyperplanes using the Möbius inversion method, the character tables and then finally the generating functions for the face colorings of the  $n$ -cube. We note that the same codes could be used for other hyperplanes of the  $n$ -cube such as vertices, edges, cells, tesseracts, and so forth. All of the computations were carried out in quadruple precision (Real\*16) arithmetic with an accuracy of up to 32 digits. We note that the needed multinomials for the colorings were computed recursively prior to constructing the GFs and stored in memory for subsequent computations of the GFs of each IR of the  $n$ -cube.

### 3. Results and Discussions

#### A. n-cube dice and chirality.

We start with the 4-cube or tesseract to illustrate the dice enumeration in fourth dimension and their chirality. The number of faces of the 4-cube and the order of the 4-cube hyperoctahedral group are 24 and 384, respectively. The generating functions can be derived from the cycle indices for the totally symmetric and chiral representations of the 4-cube which are shown below:

$$P_{S_4[S_2]}^{A_1} = \frac{1}{384} \{s_1^{24} + 4s_1^{12}s_2^6 + 6s_1^4s_2^{10} + 12s_1^6s_2^9 + 12s_1^4s_4^5 + 4s_2^{12} + 24s_1^2s_2^{11} + 24s_2^2s_4^5 + 32s_3^8 + 32s_6^4 + s_2^{12} + 12s_1^2s_2^{11} + 12s_2^2s_4^5 + 32s_3^4s_6^2 + 32s_6^4 + 12s_1^4s_2^{10} + 24s_1^2s_2^{\square} s_4^5 + 12s_4^6 + 48s_2^2s_4^5 + 48s_8^3\}$$

$$P_{S_4[S_2]}^{A_3} = \frac{1}{384} \{s_1^{24} - 4s_1^{12}s_2^6 + 6s_1^4s_2^{10} + 12s_1^6s_2^9 - 12s_1^4s_4^5 - 4s_2^{12} - 24s_1^2s_2^{11} + 24s_2^2s_4^5 + 32s_3^8 - 32s_6^4 + s_2^{12} + 12s_1^2s_2^{11} - 12s_2^2s_4^5 - 32s_3^4s_6^2 + 32s_6^4 + 12s_1^4s_2^{10} - 24s_1^2s_2^{\square} s_4^5 + 12s_4^6 + 48s_2^2s_4^5 - 48s_8^3\}$$

As the maximum of different colors that can be used to color the faces of the 4-cube is 24 the generating functions for the totally symmetric and chiral representations are obtained by replacing every  $s_k$  by

$$(\lambda_1^k + \lambda_2^k + \dots + \lambda_{23}^k + \lambda_{24}^k)$$

Thus the GF contains all possible color distributions for coloring the faces of the 4-cube such that the coefficient of a typical term  $(\lambda_1^{n_1}\lambda_2^{n_2}\dots\lambda_p^{n_p})$  in the GF gives the number of irreducible representations that occur in the set of colorings with  $n_1$  colors of type 1,  $n_2$  colors of type 2, and so forth. In particular as every face of the 4-cube needs to be colored with a different color for the dice enumeration, the coefficient of  $(\lambda_1^{\square}\lambda_2^{\square}\dots\lambda_{24}^{\square})$  in the GF enumerates the number of colorings that transform in accord with the irreducible representation. It can be seen for the 4-cube these numbers for the  $A_1$  and  $A_3$  IRs are given by

$$N_{A_1} = N_{A_3} = \left\{ \frac{1}{384} x \frac{24!}{1!1!\dots1!} \right\} = 1.61575104618031104 \times 10^{21}$$

suggesting that all 4-cube dice are chiral and there are  $1.61575104618031104 \times 10^{21}$  pairs with the total number of 4-cube dice enumerated as  $3.23150209236062208 \times 10^{21}$ .

Table 1 shows the number of dice for n-cube for n up to 7. As seen from Table 1 there are only 30 possible dice for the ordinary cube in 3-dimension all of which are chiral or equivalently there are 15 chiral pairs of cubic dice. These numbers increase in astronomical proportions as a function of n, as seen from Table 1. The number of dice in the fourth dimension already reaches  $3.23150209236062208 \times 10^{21}$  in comparison to molecular Avogadro number of  $6.023 \times 10^{23}$ . The number of dice reaches  $2.8214838544319294796427515741969896 \times 10^{1604}$  in the 7<sup>th</sup> dimension beyond which even in REAL\*16 arithmetic precision the numbers become too large to be exactly listed although the

mathematical expression for the number of chiral pairs of dice for any n-cube is derived from the GF of the n-cube as

$$N_c = \frac{\{n(n-1)2^{n-3}\}!}{n!2^n} = \frac{(n-1)!2^{n-3}!}{2^n}$$

Although this number grows astronomically natural log of the above number can be simplified using Stirling’s approximation as

$$\ln(N_c) = (n - 1) \ln(n - 1) - n + 1 + \{(n - 3)2^{(n-3)} - n\} \ln(2) - 2^{(n-3)}$$

**Table 1.** Number of possible dice in n-dimensions for n-cubes with all different numbers placed on the faces of the n-cube for n=3 to 7.

n	Faces	No of dice	No of Chiral Pairs of dice
3	6	30	15
4	24	$3.23150209236062208 \times 10^{21}$	$1.61575104618031104 \times 10^{21}$
5	80	$3.7275758878262397028547673814159646 \times 10^{115}$	$1.8637879439131198514273836907079823 \times 10^{115}$
6	240	$1.7655752446384800870197812159231254 \times 10^{464}$	$8.827876223192400435098906079615627 \times 10^{463}$
7	672	$2.8214838544319294796427515741969896 \times 10^{1604}$	$1.4107419272159647398213757870984948 \times 10^{1604}$

Given the large number of possible dice even in the fourth dimension (~1.616x10<sup>21</sup> chiral pairs of dice) the n-cube dice offer a very good platform for cryptographic applications where for example 24 faces of the 4-cube can be used to label different fragments of messages or alphabets. Moreover several such 4-cube packets can be generated to encrypt and decrypt messages using artificial intelligence techniques as we discuss in a subsequent section. For several chemical and biological applications natural log of the enumerated numbers are relevant and these number are still under control for the n-cubes. For example, entropies and information content based on dice enumerations would be measured using natural logarithms of the combinatorial numbers enumerated above.

**B. n-cube 4-color problem: dice enumeration with 4 colors for the n-cube and their chirality.**

We consider the special case of a four-color dice as the four-color problem in combinatorics and topology is quite significant. For this special case, we take a n-cube dice with 4 different colors say, green, red, violet and blue. For such a case, the combinatorics results in a generating function involving partitions with 4 parts. This is exemplified in Table 4 for a 4-cube with 24 faces four-color problem for both achiral and chiral combinatorial enumerations.

**Table 2.** The Four-Color problem of n-cube: Enumerations for the face-colorings of the 4-cube with 4 different colors. The color partition n<sub>1</sub> n<sub>2</sub> n<sub>3</sub> n<sub>4</sub> represents a coloring in which n<sub>1</sub> red, n<sub>2</sub> blue, n<sub>3</sub> green and n<sub>4</sub> yellow colors are used to color 24 faces of the 4-cube.

Color Partition	No of A <sub>1</sub> Colorings <sup>a</sup>	No of A <sub>3</sub> Colorings <sup>a</sup>
24 0 0 0	1	0
23 1 0 0	1	0
22 2 0 0	5	1
21 3 0 0	16	6
20 4 0 0	57	27



19 5 0 0	169	105
18 6 0 0	475	335
17 7 0 0	1099	866
16 8 0 0	2234	1849
15 9 0 0	3843	3307
14 10 0 0	5669	4967
13 11 0 0	7132	6336
12 12 0 0	7725	6871
22 1 1 0	5	1
21 2 1 0	32	13
20 3 1 0	158	97
19 4 1 0	688	503
18 5 1 0	2396	1973
17 6 1 0	6893	6025
16 7 1 0	16303	14810
15 8 1 0	32156	29818
14 9 1 0	53118	49918
13 10 1 0	74020	70054
12 11 1 0	87278	82892
20 2 2 0	244	145
19 3 2 0	1331	1021
18 4 2 0	5871	4986
17 5 2 0	20208	18285
16 6 2 0	56090	52312
15 7 2 0	126548	120340
14 8 2 0	235721	226411
13 9 2 0	365096	353006
12 10 2 0	473741	459377
11 11 2 0	516370	501374
18 3 3 0	7674	6682
17 4 3 0	33276	30591
16 5 3 0	110825	105097
15 6 3 0	292629	281871
14 7 3 0	623256	606096
13 8 3 0	1087220	1062760
12 9 3 0	1567505	1536897
11 10 3 0	1879494	1845178
16 4 4 0	138453	131493
15 5 4 0	437694	423510
14 6 4 0	1087993	1062443
13 7 4 0	2168246	2129446
12 8 4 0	3517231	3464261

11 9 4 0	4684708	4622058
10 10 4 0	5152084	5085022
14 5 5 0	1303756	1275752
13 6 5 0	3031508	2983480
12 7 5 0	5618270	5548102
11 8 5 0	8418614	8328046
10 9 5 0	10284396	10182022
12 6 6 0	6553122	6474210
11 7 6 0	11217872	11108824
10 8 6 0	15415306	15281078
9 9 6 0	17123720	16981820
10 7 7 0	17611556	17467588
9 8 7 0	22006070	21840340
8 8 8 0	24753462	24573093
21 1 1 1	51	22
20 2 1 1	425	281
19 3 1 1	2510	2015
18 4 1 1	11325	9945
17 5 1 1	39621	36528
16 6 1 1	110649	104649
15 7 1 1	250736	240748
14 8 1 1	467930	453070
13 9 1 1	725780	706350
12 10 1 1	942226	919270
11 11 1 1	1027332	1003242
19 2 2 1	3756	3061
18 3 2 1	22360	20105
17 4 2 1	98101	92141
16 5 2 1	329008	316265
15 6 2 1	871348	847760
14 7 2 1	1859676	1822056
13 8 2 1	3247280	3194050
12 9 2 1	4684626	4618066
11 10 2 1	5618508	5544042
17 3 3 1	130170	123075
16 4 3 1	546260	528355
15 5 3 1	1736268	1699440
14 6 3 1	4325880	4260540
13 7 3 1	8634420	8534760
12 8 3 1	14016130	13881320
11 9 3 1	18677240	18517190
10 10 3 1	20541952	20371606

15 4 4 1	2169038	2125858
14 5 4 1	6481828	6396668
13 6 4 1	15094180	14950100
12 7 4 1	28000166	27789946
11 8 4 1	41975340	41705670
10 9 4 1	51289438	50984818
13 5 5 1	18105486	17944878
12 6 5 1	39180892	38920964
11 7 5 1	67120260	66760032
10 8 5 1	92260524	91821066
9 9 5 1	102499670	102032840
11 6 6 1	78296512	77897372
10 7 6 1	122981972	122455864
9 8 6 1	153698290	153094910
9 7 7 1	175633880	174981580
8 8 7 1	197572890	196868820
18 2 2 2	33487	30322
17 3 2 2	194912	185257
16 4 2 2	818481	794136
15 5 2 2	2602172	2552704
14 6 2 2	6484766	6397066
13 7 2 2	12945012	12811992
12 8 2 2	21015167	20835247
11 9 2 2	28004836	27791786
10 10 2 2	30801270	30574296
16 3 3 2	1088655	1059945
15 4 3 2	4328656	4259696
14 5 3 2	12944976	12809676
13 6 3 2	30156640	29928140
12 7 3 2	55953912	55621272
11 8 3 2	83891030	83464690
10 9 3 2	102511416	102030166
14 4 4 2	16176465	16017675
13 5 4 2	45209956	44913056
12 6 4 2	97864801	97385171
11 7 4 2	167678736	167016576
10 8 4 2	230502306	229694856
9 9 4 2	256090630	255234030
12 5 5 2	117411604	116879096
11 6 5 2	234687752	233871724
10 7 5 2	368679660	367606632
9 8 5 2	460789280	459559450

10 6 6 2	430095214	428905586
9 7 6 2	614294660	612823960
8 8 6 2	691047030	689459130
8 7 7 2	789709860	787996500
15 3 3 3	5765010	5682726
14 4 3 3	21553380	21364620
13 5 3 3	60252960	59898540
12 6 3 3	130442733	129871167
11 7 3 3	223512780	222722100
10 8 3 3	307264170	306301230
9 9 3 3	341378584	340355686
13 4 4 3	75302150	74889430
12 5 4 3	195601766	194861566
11 6 4 3	391016740	389884220
10 7 4 3	614296776	612807816
9 8 4 3	767787880	766082150
11 5 5 3	469162776	467900988
10 6 5 3	859878528	858043860
9 7 5 3	1228207740	1225936680
8 8 5 3	1381679430	1379231310
9 6 6 3	1432840398	1430330262
8 7 6 3	1842059400	1839135600
7 7 7 3	2105109000	2101948920
12 4 4 4	244472700	243610770
11 5 4 4	586400958	584936118
10 6 4 4	1074771633	1072641603
9 7 4 4	1535163270	1532530170
8 8 4 4	1726995915	1724156055
10 5 5 4	1289616636	1287246912
9 6 5 4	2148984460	2145744020
8 7 5 4	2762767590	2758994670
8 6 6 4	3223114485	3218943735
7 7 6 4	3683411640	3678907800
9 5 5 5	2578619766	2575009806
8 6 5 5	3867527364	3862884864
7 7 5 5	4419870336	4414853016
7 6 6 5	5156360952	5150820912
6 6 6 6	6015584844	6009464868

<sup>a</sup>N(A<sub>1</sub>)+ N(A<sub>3</sub>) yields the total number of colorings among which N(A<sub>3</sub>) enumerate chiral pairs.

C. Chess Board type Black and white dice enumeration in n dimension and their chirality.

In this section we consider a black-and-white dice combinatorics akin to that of a chess board. For this purpose, we take a 6-cube shown in Figure 2, although we consider the faces of the 7-cube. The generating functions were computed for both totally symmetric and chiral representations for the binomial distribution. The results were computed in quadruple precision and are shown in Table 3 for coloring 240 faces of the 6-cube with black and white colors. We have restricted listing the computed results only for the totally symmetric  $A_1$  irreducible representation. It is pointed out that almost all colorings become chiral when the colorings are evenly distributed culminating into a maximum for 120 black and 120 white colors for coloring 240 faces of a 6-cube.

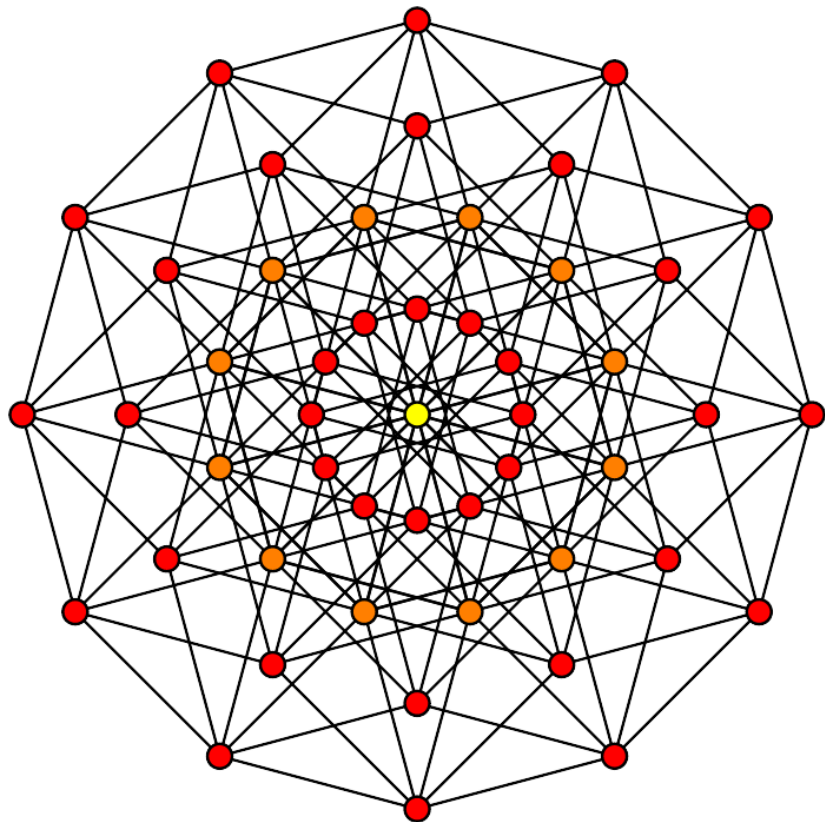


**Figure 2.** Graphical representation of hexeract or 6-cube. Table 3 enumerates black & white face colorings of the 6-cube with varied number of black and white colors, Reproduced from [60].

**Table 3.** Black-and White dice of hypercube in the 6<sup>th</sup> dimension with 240 faces;  $n_b$  stands for the number of black colors with  $240-n_b$  being the number of white colors.

$n_b$	$N(A_1)$
0	1
1	1
2	11
3	139
4	4176
5	152635
6	5580266
7	182586993



8	5283117184
9	135891832431
10	3136801139463
11	65570741043751
12	1251192201334018
13	21943233858075034
14	355789263949855043
15	5360531557936453701
16	75382327861202736302
17	993272251366379046339
18	12305535660981459650639
19	143780450498062303705832
20	1588773890867771345864514
21	16644297515678879808798297
22	165686414507591622101552686
23	1570419052306115065132618723
24	14199205570066871577428871140
25	122681136017010754158309432703
26	1014478624347489084027884140426
27	8040682428518284564435181330429
28	61166619897340434689394786752894
29	447149083369066948751292268832796
30	3144948552967196406093283337735784
31	21304490197316629654279247580024508
32	139144951600574592746649080159671056
33	877034846450078628652128896100267264
34	5339594506322238375552079147434465280
35	31427327665763904958336467271605932032
36	178961171429990835258310915317808332800
37	986704837073310196335657862006172680192
38	5271081103312257287838648872443980546048
39	27301496996641809668910837171761665015808
40	137190022408121978237796878411228575170560
41	669219621503025866250112350741134231732224
42	3170826301883363428193286508672704248283136
43	14600549017974504078101835470726548970012672
44	65370639921385716211126737122035700519141376
45	284725453879813021523275240995846178515976192
46	1206988337099206608564703950062943154911313920
47	4982036965898851012606659737835556794489896960
48	20031940300384959298052361807805291335079952384
49	78492500768855341303876241965943810733935427584

50	299841352937027382765902773445578163675698561024
51	1117056020745788242590376169881100544777740353536
52	4060068998479884089705015623755515419238105874432
53	14401754183287135804246166953385408335748576313344
54	49872741338420266137322529195039577022891227611136
55	168660543435384899112410284701246690287995790032896
56	557182152420467968422421922547752056414106468483072
57	1798623088515194841712775021084035912510703835021312
58	5674965951694494062205410635512839112833661296181248
59	17505827173023693533563297554260934909613741294223360
60	52809245305288142132272869107153182169520534320054272
61	155830559917243698043653761141737793516691944388952064
62	449897906857848741029976049141268839915375321375834112
63	1271140117788842474479687792473475435071770769766744064
64	3515496888259767468163216556014840184143394537746726912
65	9518883882057216528608998367914143748380503439084355584
66	25239464838788074127879708050806830413286976339971145728
67	65547266894763058181097740456058221177846743153120378880
68	166759958423441309781250299599634334821117425640231927808
69	415691490562781235971341064888171821804599513259251335168
70	1015474926946222733578581339228367257143428701318056771584
71	2431418839167012178976836276667886688093053146703593472000
72	5707080330822570253408677742000332960960832242019794419712
73	13134102679153312363971846877730573818996158520436289699840
74	29640474965116258983498939796906579169557606545381706956800
75	65604251256123986550051347634863006077799034966669772455936
76	142430282332374444483519754796895120849199732824551463059456
77	303358003928693622016625857618977262242204533973550601601024
78	633940444107398210111331355025827016639517714599813255790592
79	1299979138549348228329063291451252319874543714414110345003008
80	2616208016330563309511496917583731993831663122674685994598400
81	5167818303862841105206809240136218974660614845481150429790208
82	10020525735538923606436025159797456261476584970542687191040000
83	19075217665242770238755496178613251023787049655038318777204736
84	35652490160037082470051758173077553030081498177735400332722176
85	65432805470185704297972943306063050464253178396461240116314112
86	117931219161381211234712613738006405558219054813035950984134656
87	208751813228192029082126716097532138898293814638576077423771648
88	362943493453561141472322840478800602327652562685480290771533824
89	619858550617317904536986031056340852095924421733185407357550592
90	1039984901591277817612034918976099698126465664356715106718973952
91	1714260826798809589470361996501267583138843705609748724712472576

92	2776357208619811182946532139254981696976848855712642666273439744
93	4418288891136903818022397130640910763680489058711583357765943296
94	6909451776565158098396675870686568083843531086171523326916165632
95	10618736414510664024904301130552081477721498205603021838987821056
96	16038716459417148787615793261697627570544461777441421000234237952
97	23810053300578035313573866471631103862233086767820943288313053184
98	34743241040639378059602569562006314113107754712353068755277840384
99	49833739674452441257207592441071504972429917631360631482888486912
100	70265572940977942172662549542368590308742746503025565569864695808
101	97397823878583286179928107075659666820641201605644990708709326848
102	132728407050226242931470451731079405476392486433062572665908232192
103	177830292941079820626630085054867470806112050016763218951307001856
104	234257212816614763710079762418248667308011746087552551552313982976
105	303418866124377217757817320211010493225990120075604352544075153408
106	386429687988593626389672704093941308509024324478124575046739427328
107	483939983088519120899215967419979205493870806825180030389467480064
108	595963127321972621107367481426572082532281766779222667980204670976
109	721716814738535651249288720668083207973311214195686476972126371840
110	859499115734074275578698042830041010298057135266173370496370868224
111	1006620585994861764191267638613753417255640297161311448121542180864
112	1159411210654796139113156147343784043908458958128856461986303574016
113	1313315353662069962889238509921566661821965008467180176968339423232
114	1463079385220025309534502263293078969347233893342480581579761516544
115	1603026109023679904359541354461619193561740429737992388679403831296
116	1727398824378965414180540034621696361312587920268799182661767659520
117	1830747471991382148362281571140508950236269928271495714066772525056
118	1908321517414745798716615408358714803655391352966327587613939073024
119	1956430463231924264230479584872704778184154074936145924234846142464
120	1972734050425523633099066888879877060171554196485690791403223777280

D. Rubik’s Cube Enumerations and colorings.

Rubik’s cube [61] is an interesting case of hypercube and hyperoctahedral symmetry, as it has been a cynosure of puzzles and games over four decades. The symmetry operations of a Rubik’s cube can be rationalized by dividing the cubes to corner cubes and edge cubes. As seen from Figure 3, which shows a typical Rubik’s cube, the eight corner cubes carry three faces while the 12 edge cubes carry 2 faces each. The dynamics of the Rubik’s cube facilitates three fold rotations of each corner cube independent of other cubes while providing two fold flipping motions of the edge cubes. The eight corners of the overall cube can be permuted in all possible ways with each cube within each corner undergoing a three-fold rotation during various dynamical operations of the Rubik’s cube. Likewise the twelve edge cubes can be permuted in all possible ways with each cube within the edge exhibiting a two-fold flip. This results in the direct product of two hyperoctahedral groups, namely, the corner cubes generating the  $S_8[C_3]$  wreath product while the edge cubes give rise to the wreath product  $S_{12}[S_2]$ . Consequently, the overall group of the Rubik’s cube is the direct product  $S_8[C_3] \times S_{12}[S_2]$ . The cubes within the Rubik’s cube are partitioned into three classes, 8 corner cubes,

12 edge cubes and 6 center cubes. Consequently, the 54 faces of the Rubik's cube are partitioned into 24 corner square faces, 24 edge square faces and 6 central square faces. The overall order of Rubik's cube group is obtained by multiplying the orders of comprising wreath product groups yielding  $5.19024039293878272 \times 10^{20}$  symmetry operations in the Rubik's cube.

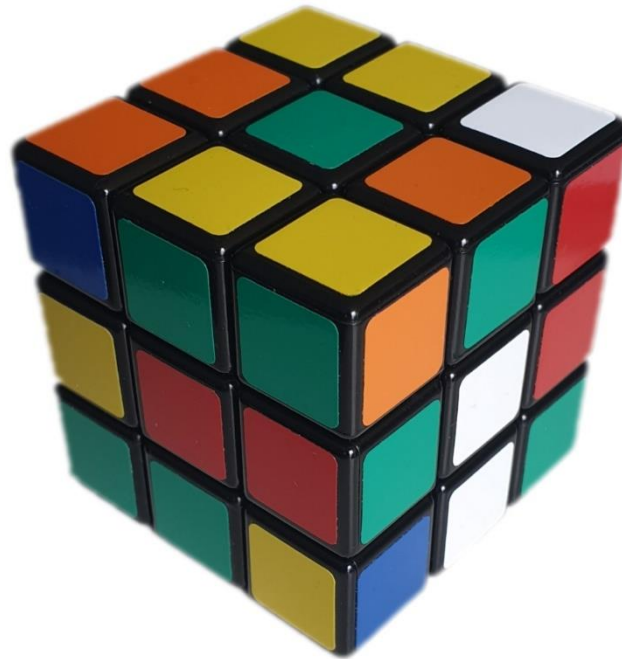


**Figure 3.** Rubik's Cube: There are  $5.34018574959804633194496 \times 10^{29}$  possible dice for Rubik's cube, see text for details of enumeration. Reproduced from [62].

Hence we arrive at the result for the number of dice that can be obtained by using distinct numbers for each of the corner faces, edges faces and central faces, that is, treating the set of faces in the three partitions independent of each other as

$$N_c = \frac{24!24!6!}{12!x8!x3^8x2^{12}} = 5.34018574959804633194496 \times 10^{29}$$

In the above enumeration, analogous to previous enumerations considered in this study, we treat the faces that are not equivalent separately rather than all faces of the object collectively. This is made possible by the equivalence classes of face partitions generated by the overall group, and consequently, two faces in different classes are never permuted into each other by any of the symmetry operations.

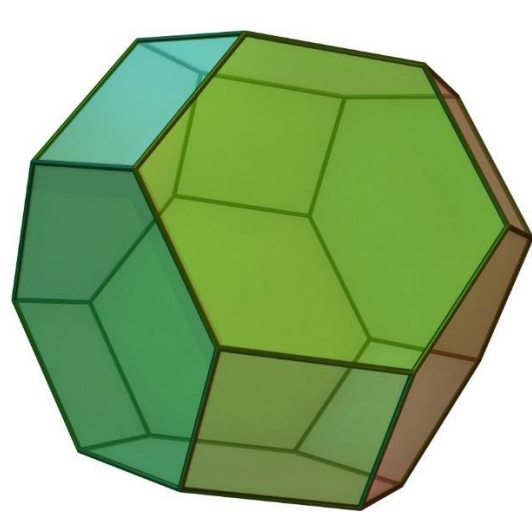
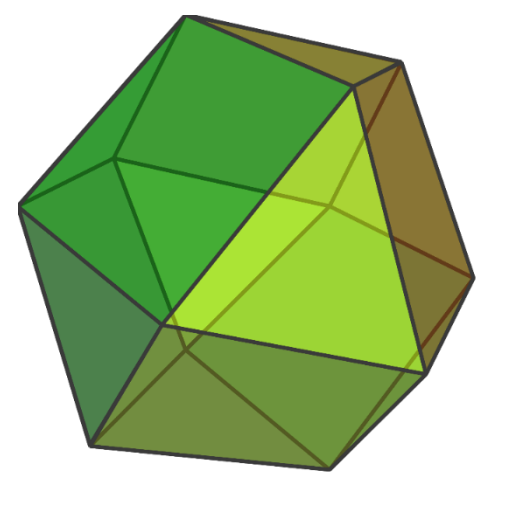
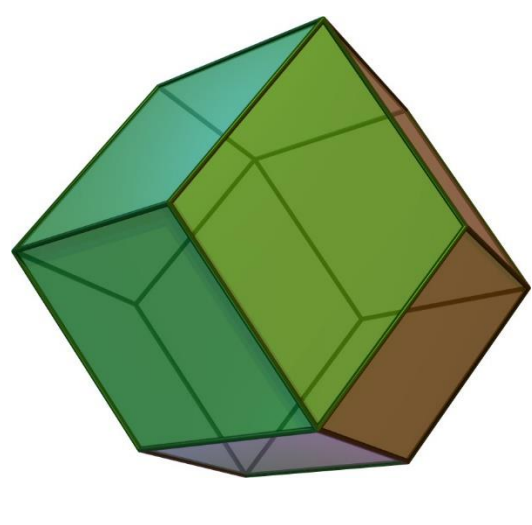
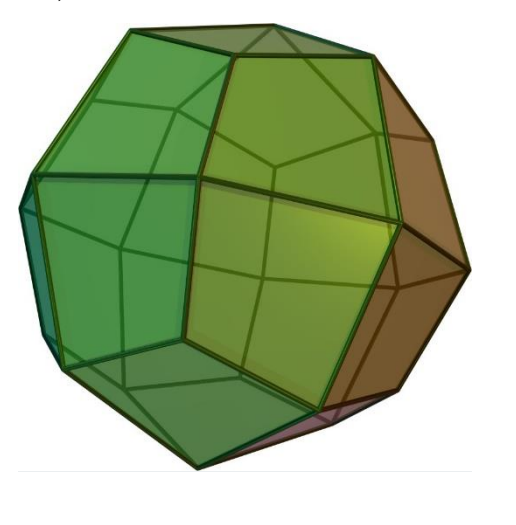
#### E. Dice of different shapes with octahedral/cubic symmetries.

Next we consider dice that can be constructed with several shapes of octahedral or cubic symmetries and that which are not comprised of the regular cubes of normal dice. Such dice enumerations not only generalize the normal cubic dice shapes but also pave the way for several applications in a variety of fields. Stimulated by such applications and mathematically intriguing nature and aesthetics of these shapes, we have shown in Table 4, a collection of dice of varied shapes, a common feature being their symmetries are all described by the octahedral group  $O_h$  containing 48 operations with the exception of the snubcube which is chiral with the symmetry group  $O$ .

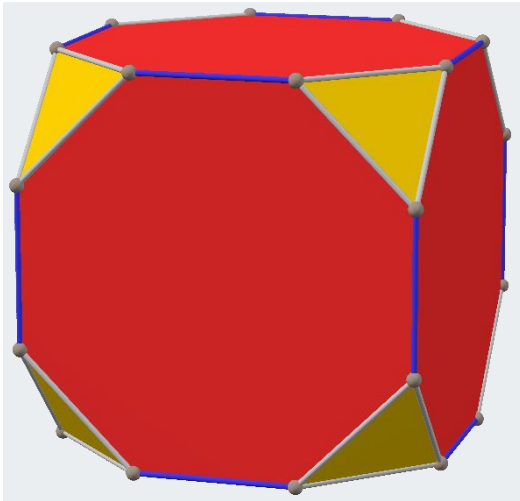
Table 4 considers several shapes of octahedral or cubic symmetries many of which are not only mathematically interesting but have several applications to materials such as zeolites and

mesoporous molecular sieves. The combinatorial enumerations considered in Table 4 make use of face partitions. That is, faces of different shapes, for examples, squares and hexagons of a truncated octahedron are treated as different equivalence classes and thus they are not treated as a single entity in the combinatorial enumeration. This is the case in many practical applications as a hexagonal face capping is not equivalent to a square face capping in molecular structures. Thus eight hexagons and 6 squares are treated as separate equivalence classes in dice enumerations of a truncated octahedron dice shown in Table 4. .

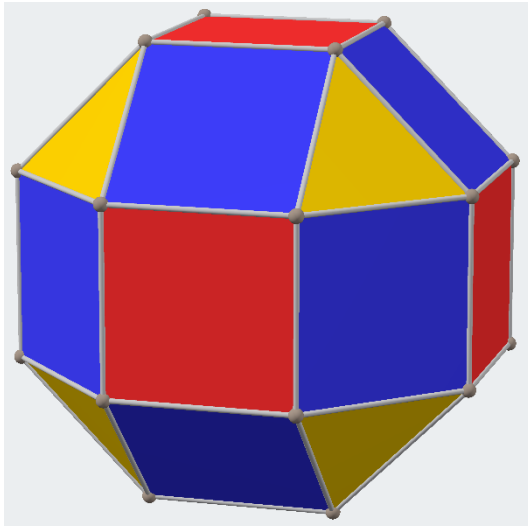
**Table 4.** Combinatorial Enumeration of dice of different shapes with Octahedral/cubic Symmetries<sup>a</sup>.

	
Truncated octahedron 604,800 Chiral Pairs of dice	Cuboctahedron (isochiral with truncated octahedron) 604,800 Chiral Pairs of dice
	
Rhombicdodecahedron 1,816,214,400 Chiral Pairs of dice	<b>deltoidal icositetrahedron</b> 133,382,785,536,000 Chiral Pairs of dice

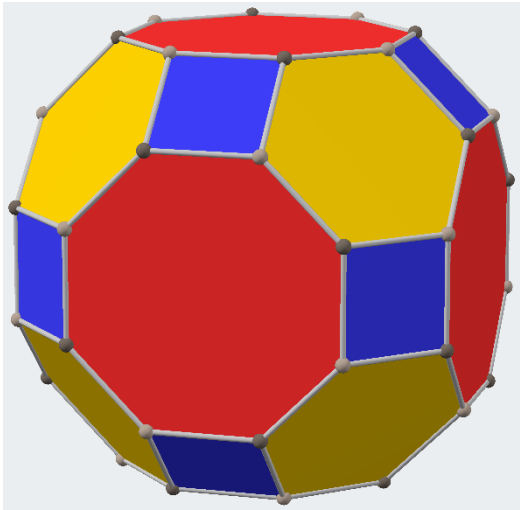




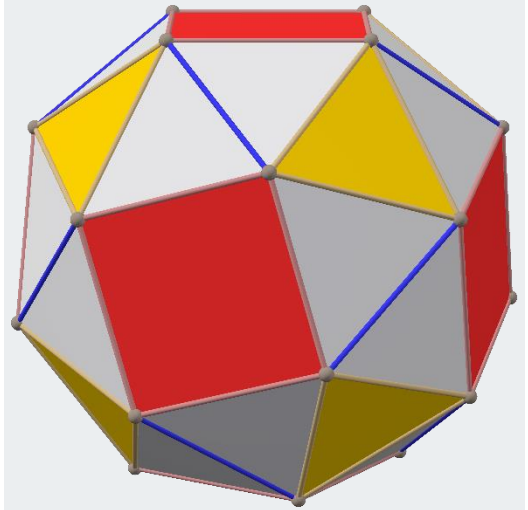
Truncated Cube:  $6!8!/48$   
604,800 Chiral pairs of dice  
isochiral with truncated octahedron



Rhombic cuboctahedron:  $6!12!8!/48$   
289,700,167,680,000 Chiral Pairs of dice



Truncated cuboctahedron 289,700,167,680,000  
Chiral Pairs  
of dice: Isochiral with Rhombic cuboctahedron.



Suncube(chiral)  
 $7.8939251080108059050165403648 \times 10^{36}$

<sup>a</sup>All Images were created by POV-RAY codes and are public domain open-access freely reproduced from ref [63].

There are a few interesting findings that emerge from a critical analysis of Table 4. First all dice enumerated in Table 4 are chiral and hence we list the number of dice as chiral pairs of dice. We label the faces in different equivalence classes with numbers 1 through  $|C|$ , where  $|C|$  is the cardinality of the equivalence class C. Although with the exception of the suncube, the parent structures shown in Table 4 are not chiral, the dice originating from every shape are chiral. The suncube is an interesting case of octahedral symmetry as the structure itself is chiral as its symmetry group is  $O$  rather than  $O_h$ . All other structures in Table 4 conform to  $O_h$  symmetry.

As can be seen from Table 4, there exists two different structures with the same chiral pairs of dice. For example, truncated cuboctahedron exhibits the same number of chiral pairs of dice as rhombic cuboctahedron (See Table 4). We call such structures with different shapes with the same number of chiral pairs of dice as isochiral. In some cases isochirality arises from mapping the vertices

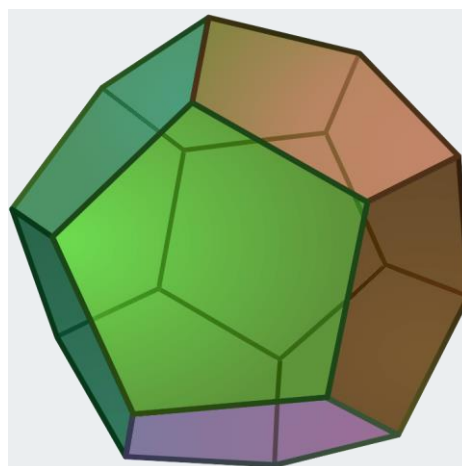
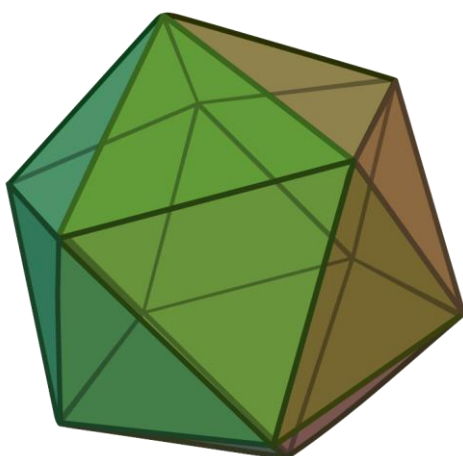
of an octahedron with different shapes of faces while in other cases it is quite interesting in that the number of faces is not even the same. For example, the truncated cuboctahedron can be obtained by mapping the red squares of the rhombic cuboctahedron with decagons and triangles with hexagons. Thus isochirality can be readily explained for such direct topological transforms. On the other hand, the isochirality of a cuboctahedron and truncated octahedron is less obvious from a simple observation. These enumerations and the chirality aspects of the enumerated structures open up a plethora of applications to a number of fields as we discuss subsequently.

#### F. Enumeration of Dice and face colorings of different shapes with icosahedral symmetries.

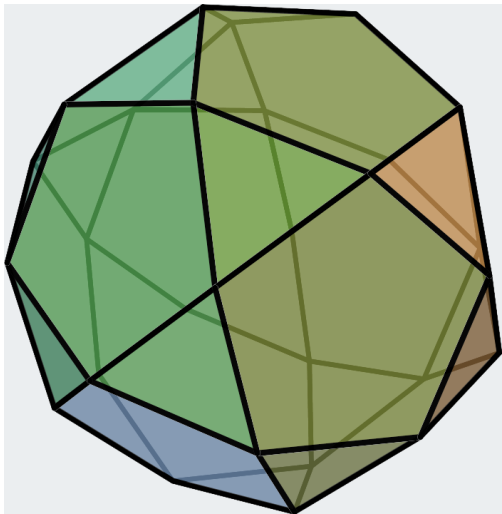
Icosahedral symmetries are quite interesting as demonstrated earlier [3,65] in that the character values of the three dimensional irreducible representations of the  $I_h$  group are golden ratios or their reciprocals thus making them interesting candidates for symmetry studies. Furthermore icosahedral symmetries occur in the molecular structures of boranes, carboranes, and metallocarboranes as well as the celebrated buckminsterfullerene,  $C_{60}$  which became the subject matter of the Nobel prize winning work of Smalley and coworkers [66,67]. Hence we devote this subsection to different shapes of icosahedral symmetries.

Table 5 shows a number of structures with icosahedral symmetry ( $I_h$ ) starting with the regular icosahedron itself which consists of 20 triangles. Many of the structures in Table 5 are Archimedean solids and share the same symmetry group. They differ in number of faces or the shapes of the faces. While the icosahedron contains 20 triangles the relative dodecahedron contains 12 pentagons (see Table 5). Consequently, the number of chiral pairs of dice for an icosahedron is considerably larger (20,274,183,401,472,000) compared to 3,991,680 chiral pairs for a dodecahedron. This can be envisaged by mapping the 12 vertices of the icosahedron into pentagons which generates the dodecahedron. Thus the dice enumeration of dodecahedron is equivalent to the vertex coloring problem of icosahedron with 12 different colors. As can be seen from Table 5, Icosododecahedron and truncated dodecahedron are isochiral as they both generate  $9.7113662879985303552 \times 10^{24}$  chiral pairs of dice. Likewise there are a number of isochiral pairs of structures in Table 5. For example, truncated icosododecahedron and rhombicosidodecahedron are isochiral. The truncated icosododecahedron has also been considered in molecular context as a candidate for the structure of  $C_{120}$  and it has been called archimedene [68]. The spectra, characteristic polynomials and other graph theoretical properties of archimedene and related clusters have been considered before [68]. The truncated icosahedron shown in Table 5 is of special interest in the context of fullerenes which are structures containing 12 pentagons and any number of hexagons. As seen from Table 5, the structure which is the molecular structure of  $C_{60}$  Buckminsterfullerene exhibits  $9.7113662879985303552 \times 10^{24}$  chiral pairs of dice.

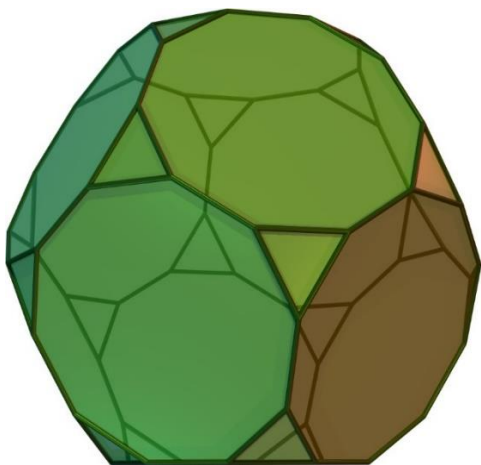
**Table 5.** Combinatorial Enumeration of dice with different shapes with Icosahedral Symmetry. <sup>a</sup>.



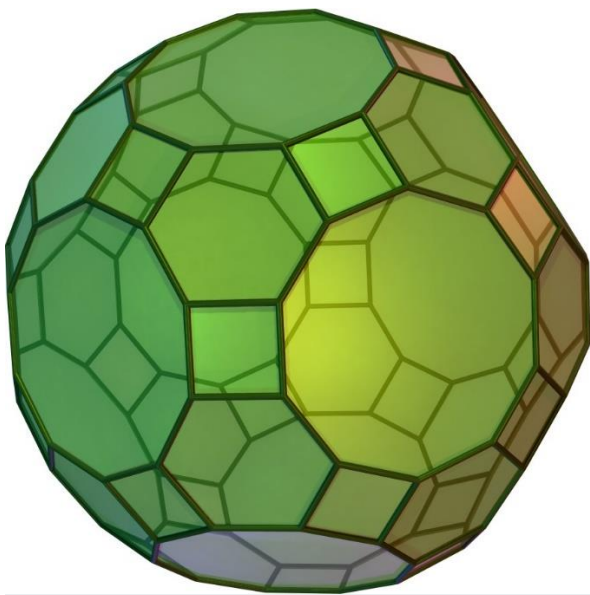
Icosahedron: Chiral Pairs of Dice:  
20,274,183,401,472,000



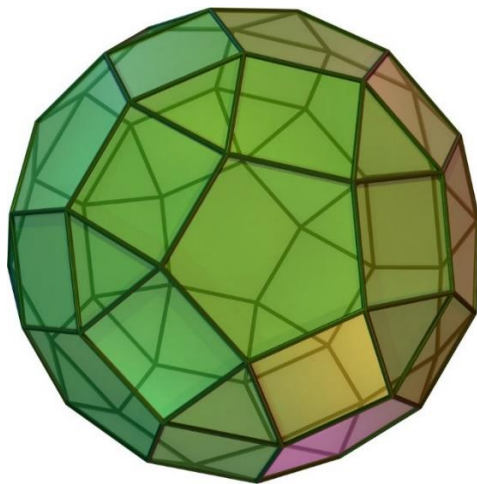
Dodecahedron: 3,991,680 Chiral Pairs of  
Dice



Icosododecahedron  $9.7113662879985303552 \times 10^{24}$   
chiral pairs of dice

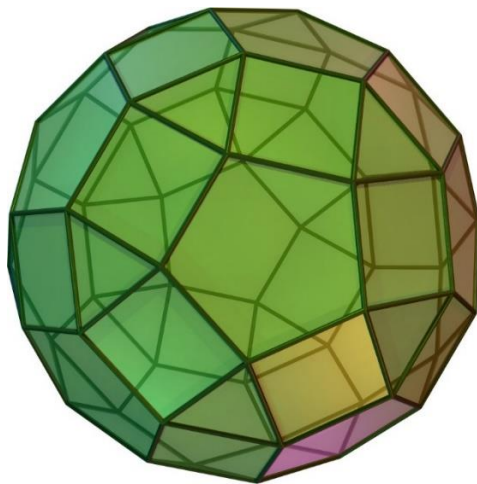


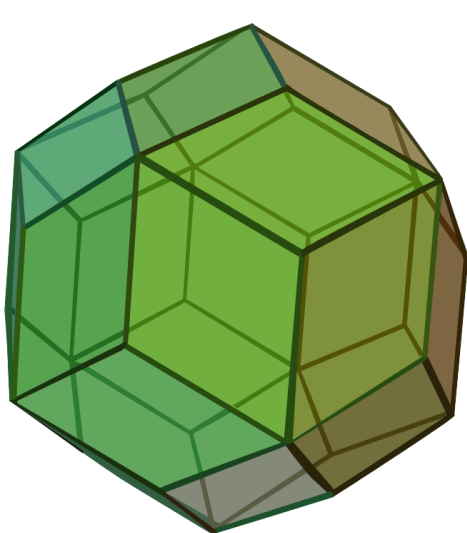
Truncated dodecahedron:  
 $9.7113662879985303552 \times 10^{24}$  chiral pairs  
of dice



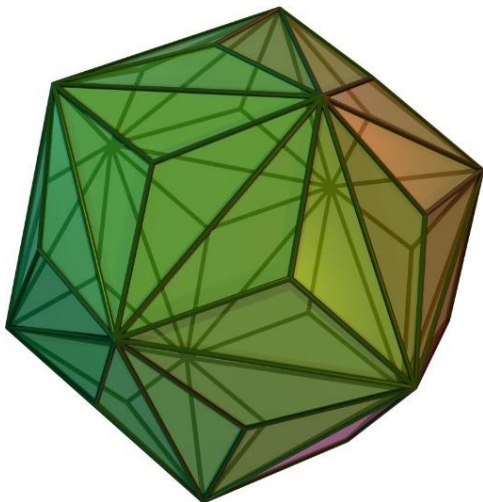
Truncated icosodedecahedron  
 $2.5759676805753124307695693098745908 \times 10^{57}$  chiral  
pairs of dice

Rhombicosidodecahedron:  
 $2.5759676805753124307695693098745908 \times$   
 $10^{57}$  chiral pairs of dice

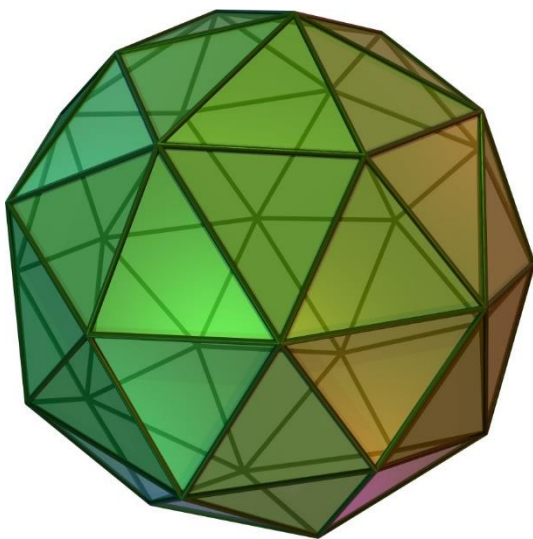




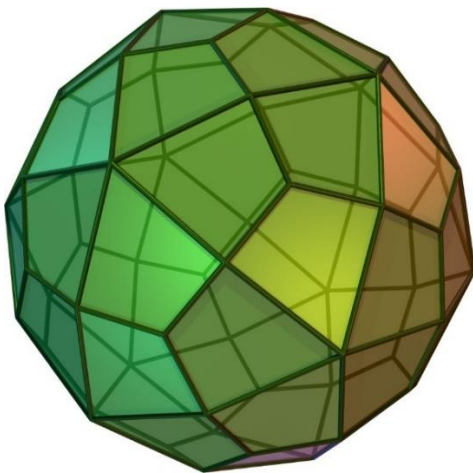
rhombic triacontahedron :  
2.210440498434925488635904x 10<sup>30</sup> chiral pairs



triakis icosahedron  
6.93415592728449178689695098601947 x  
10<sup>79</sup>chiral pairs

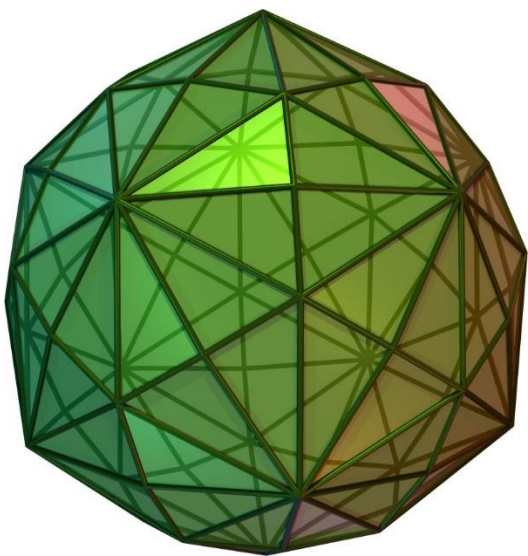


pentakis dodecahedron :  
6.93415592728449178689695098601947 x 10<sup>79</sup> chiral  
pairs



deltoidal hexecontahedron  
6.93415592728449178689695098601947 x  
10<sup>79</sup> Chiral Pairs

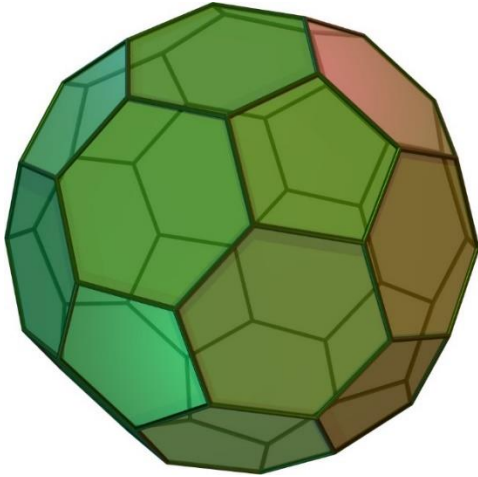




disdyakis triacontahedron:

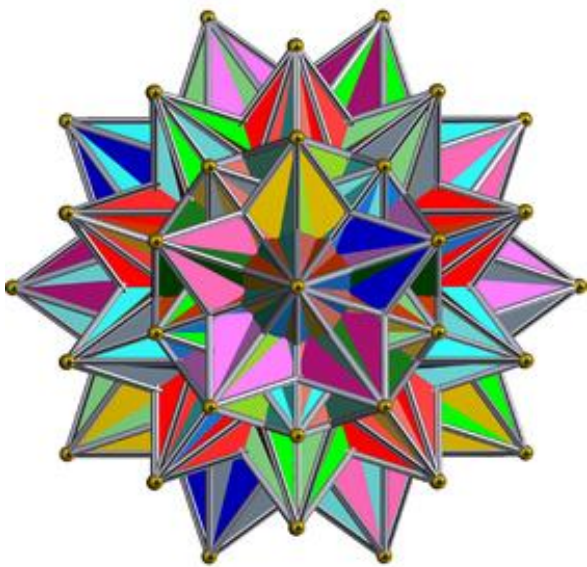
$5.574585761207605881323431711741975 \times 10^{196}$  Chiral

Pairs



Truncated icosahedron:

$9.7113662879985303552 \times 10^{24}$  chiral pairs



Grand 600-Cell/grand polytetrahedron

$4.4102702121446021496460288562760144 \times 10^{3171}$

Chiral Pairs

<sup>a</sup>All Images were created by POV-RAY codes and are public domain freely reproduced from ref [63].

The last structure shown in Table 5, the grand 600-cell or grand polytetrahedron requires further discussion as it poses grand challenge for the dice enumeration. First it contains 1200 triangular faces with a symmetry group that contains 14,400 symmetry elements which is square of the order of the icosahedral group. Consequently, the number of chiral pairs of dice for the 600-cell in Table 5 is given by



$$N_c = 1200!/14400$$

As direct computation of such a large factorial is quite difficult, we invoked Stirling’s approximation for the factorial of large numbers as follows:

$$n! \sim \sqrt{2\pi n} \left(\frac{n}{e}\right)^n \left\{1 + \frac{1}{12n} + \frac{1}{288n^2} - \frac{139}{51840n^3} - \frac{571}{2488320n^4} \dots \dots \right\}$$

Using the above approximation for n! we could compute the number of grand-600 cell dice using Fortran ’95 software in quadruple precision as

$$1200! \sim 6.350789105488227095490281553037461 \times 10^{3175}$$

And thus the number of grand cell-600 dice as

$$N_c = 6.350789105488227095490281553037461 \times 10^{3175}/14400 =$$

$$4.4102702121446021496460288562760144 \times 10^{3171}$$

The grand 600-cell is certainly a challenging object for the dice enumeration problem. Among the structures shown in Table 5, the truncated icosahedron or the structure of buckminsterfullerene can be studied further, as it poses several interesting questions and it continues to be a subject matter of active investigation. Table 6 shows the face colorings of the faces of the buckyball for coloring the hexagons with 6 different colors (vibgyr) and pentagons with 10 different colors (vibgyorbwp). We show the computed combinatorial numbers for the  $A_g$  and  $A_u$  irreducible representations for 20 hexagons and 12 pentagons, respectively. The sum of  $A_g$  and  $A_u$  numbers give the total number of inequivalent face colorings while the  $A_u$  numbers correspond to the chiral pairs. The difference between  $A_g$  and  $A_u$  numbers yield the number of achiral colorings. As seen from Table 6, as the color partition gets distributed, for example, 4 4 3 3 3 3 for the hexagons almost every hexagonal face coloring is chiral. The same comment applies to the colorings of pentagons for a distributed color partition (See, Table 6).

**Table 6.** Six-color Enumeration for hexagons & Ten-color Enumeration for Pentagons of the Buckyball: Enumeration of Chiral and achiral colorings: For hexagons of the buckyball with 6 types of colors (vibgyr)<sup>a</sup> For pentagons 10- types of colors: vibgyorbwp (b:black, w:white, p:pink).

Hexagons			Pentagons		
Color Partition	$A_g$	$A_u$	Color Partition	$A_g$	$A_u$
20 0 0 0 0 0	1	0	12 0 0 0 0 0 0 0 0 0	1	0
19 1 0 0 0 0	1	0	11 1 0 0 0 0 0 0 0 0	1	0
18 2 0 0 0 0	5	1	10 2 0 0 0 0 0 0 0 0	3	0
17 3 0 0 0 0	5	2	9 3 0 0 0 0 0 0 0 0	3	0
16 4 0 0 0 0	15	6	8 4 0 0 0 0 0 0 0 0	5	0
18 1 1 0 0 0	34	23	10 1 1 0 0 0 0 0 0 0	9	2
17 2 1 0 0 0	60	54	9 2 1 0 0 0 0 0 0 0	14	8
16 3 1 0 0 0	58	38	8 3 1 0 0 0 0 0 0 0	10	2
16 2 2 0 0 0	176	151	8 2 2 0 0 0 0 0 0 0	23	10

17 1 1 1 0 0	274	233	9 1 1 1 0 0 0 0 0 0	37	20
16 2 1 1 0 0	498	471	8 2 1 1 0 0 0 0 0 0	57	42
16 1 1 1 1 0	972	966	8 1 1 1 1 0 0 0 0 0	102	96
15 5 0 0 0 0	149	113	7 5 0 0 0 0 0 0 0 0	12	2
14 6 0 0 0 0	674	622	6 6 0 0 0 0 0 0 0 0	42	24
15 4 1 0 0 0	1337	1249	7 4 1 0 0 0 0 0 0 0	80	52
14 5 1 0 0 0	2610	2562	6 5 1 0 0 0 0 0 0 0	144	120
15 3 2 0 0 0	3928	3824	7 3 2 0 0 0 0 0 0 0	216	180
14 4 2 0 0 0	7776	7728	6 4 2 0 0 0 0 0 0 0	408	384
14 3 3 0 0 0	15504	15504	6 3 3 0 0 0 0 0 0 0	792	792
15 3 1 1 0 0	371	310	7 3 1 1 0 0 0 0 0 0	18	6
14 4 1 1 0 0	1984	1892	6 4 1 1 0 0 0 0 0 0	58	36
15 2 2 1 0 0	4984	4796	7 2 2 1 0 0 0 0 0 0	142	104
14 3 2 1 0 0	9744	9636	6 3 2 1 0 0 0 0 0 0	246	216
14 2 2 2 0 0	6557	6373	6 2 2 2 0 0 0 0 0 0	178	134
15 2 1 1 1 0	19480	19280	7 2 1 1 1 0 0 0 0 0	488	436
14 3 1 1 1 0	38784	38736	6 3 1 1 1 0 0 0 0 0	936	912
14 2 2 1 1 0	29352	28968	6 2 2 1 1 0 0 0 0 0	748	668
14 2 1 1 1 1	58248	58032	6 2 1 1 1 1 0 0 0 0	1416	1356
13 7 0 0 0 0	116304	116256	5 5 2 0 0 0 0 0 0 0	2784	2760
12 8 0 0 0 0	693	609	5 4 3 0 0 0 0 0 0 0	5544	5544
13 6 1 0 0 0	4597	4457	4 4 4 0 0 0 0 0 0 0	160	118
12 7 1 0 0 0	13720	13412	5 5 1 1 0 0 0 0 0 0	296	260
13 5 2 0 0 0	27216	27048	5 4 2 1 0 0 0 0 0 0	258	204
12 6 2 0 0 0	22802	22438	4 4 3 1 0 0 0 0 0 0	726	660
13 4 3 0 0 0	68040	67620	4 4 2 2 0 0 0 0 0 0	1404	1368
12 5 3 0 0 0	135744	135576	5 4 1 1 1 0 0 0 0 0	960	888
12 4 4 0 0 0	90618	90282	4 4 2 1 1 0 0 0 0 0	1440	1332
13 5 1 1 0 0	136024	135296	4 4 1 1 1 1 0 0 0 0	2808	2736
12 6 1 1 0 0	271488	271152	5 3 3 1 0 0 0 0 0 0	5544	5544
13 4 2 1 0 0	542640	542640	5 3 2 2 0 0 0 0 0 0	4224	4092
12 5 2 1 0 0	407400	406560	4 3 3 2 0 0 0 0 0 0	8352	8280
12 4 3 1 0 0	814128	813792	5 3 2 1 1 0 0 0 0 0	16632	16632
12 4 2 2 0 0	1135	1022	4 3 3 1 1 0 0 0 0 0	33264	33264
13 4 1 1 1 0	8501	8305	5 2 2 2 1 0 0 0 0 0	330	270
12 5 1 1 1 0	29739	29262	4 3 2 2 1 0 0 0 0 0	1194	1116
12 4 2 1 1 0	58917	58665	4 2 2 2 2 0 0 0 0 0	1818	1692
12 4 1 1 1 1	59085	58497	5 2 2 1 1 1 0 0 0 0	3510	3420
11 9 0 0 0 0	176680	176036	4 3 2 1 1 1 0 0 0 0	6948	6912
10 10 0 0 0 0	352800	352632	4 2 2 2 1 1 0 0 0 0	2376	2244
11 8 1 0 0 0	74014	73286	4 2 2 1 1 1 1 0 0 0	4656	4584
10 9 1 0 0 0	294290	293590	3 3 3 3 0 0 0 0 0 0	7008	6852

11 7 2 0 0 0	441952	440468	3 3 3 2 1 0 0 0 0 0	13896	13824
10 8 2 0 0 0	882168	881412	3 3 2 2 2 0 0 0 0 0	27720	27720
11 6 3 0 0 0	1763664	1763496	3 3 2 2 1 1 0 0 0 0	10572	10308
10 7 3 0 0 0	588509	587221	3 2 2 2 2 1 0 0 0 0	20880	20700
10 6 4 0 0 0	1175898	1175562	2 2 2 2 2 2 0 0 0 0	41616	41544
11 7 1 1 0 0	1764280	1762880	3 2 2 2 1 1 1 0 0 0	83160	83160
10 8 1 1 0 0	3527328	3526992	2 2 2 2 2 1 1 0 0 0	166320	166320
11 6 2 1 0 0	2647512	2644488	2 2 2 2 1 1 1 1 0 0	3156	3012
10 7 2 1 0 0	5291496	5289984	2 2 2 2 2 2 0 0 0 0	9312	9168
10 6 3 1 0 0	1466	1340	3 3 3 1 1 1 0 0 0 0	18480	18480
10 6 2 2 0 0	12716	12478	3 3 2 2 2 0 0 0 0 0	13992	13728
11 6 1 1 1 0	50696	50080	3 3 2 2 1 1 0 0 0 0	27792	27648
10 7 1 1 1 0	100944	100608	3 3 2 1 1 1 1 0 0 0	55440	55440
10 6 2 1 1 0	118002	117162	3 3 1 1 1 1 1 1 0 0	110880	110880
10 6 1 1 1 1	353192	352240	3 2 2 2 2 1 0 0 0 0	41736	41424
9 9 2 0 0 0	705600	705264	3 2 2 2 1 1 1 0 0 0	83232	83088
9 8 3 0 0 0	176904	175812	3 2 2 1 1 1 1 1 0 0	166320	166320
8 8 4 0 0 0	705936	704928	3 2 1 1 1 1 1 1 1 0	332640	332640
9 9 1 1 0 0	1059240	1057056	3 1 1 1 1 1 1 1 1 1	665280	665280
9 8 2 1 0 0	2116800	2115792	2 2 2 2 2 2 0 0 0 0	62736	62184
8 8 3 1 0 0	4232592	4232592	2 2 2 2 2 1 1 0 0 0	124920	124560
8 8 2 2 0 0	882504	881076	2 2 2 2 1 1 1 1 0 0	249552	249408
9 8 1 1 1 0	1764840	1762320	2 2 2 1 1 1 1 1 1 0	498960	498960
8 8 2 1 1 0	3527664	3526656	2 2 1 1 1 1 1 1 1 1	997920	997920
8 8 1 1 1 1	5292168	5289312			
13 3 3 1 0 0	10581984	10580976			
13 3 2 2 0 0	2352468	2350452			
12 3 3 2 0 0	7055328	7053312			
13 3 2 1 1 0	14108640	14108640			
12 3 3 1 1 0	10584000	10578960			
13 2 2 2 1 0	21163968	21161952			
12 3 2 2 1 0	31747296	31741584			
12 2 2 2 2 0	1648	1510			
13 2 2 1 1 1	15536	15270			
12 3 2 1 1 1	69812	69070			
12 2 2 2 1 1	138756	138378			
11 5 4 0 0 0	185308	184244			
10 5 5 0 0 0	554856	553680			
11 5 3 1 0 0	1108704	1108368			
11 4 4 1 0 0	324428	322888			
10 5 4 1 0 0	1294012	1292612			
11 5 2 2 0 0	1942136	1939000			

11 4 3 2 0 0	3880632	3879120
10 5 3 2 0 0	7759920	7759584
10 4 4 2 0 0	388788	387192
10 4 3 3 0 0	1940904	1938972
11 5 2 1 1 0	3881640	3878112
11 4 3 1 1 0	7760256	7759248
10 5 3 1 1 0	11641560	11637696
10 4 4 1 1 0	23279760	23278752
11 4 2 2 1 0	4853184	4848396
10 5 2 2 1 0	9700824	9698556
10 4 3 2 1 0	6468432	6464568
10 4 2 2 2 0	19401480	19397280
11 4 2 1 1 1	38799264	38798256
10 5 2 1 1 1	29105832	29096088
10 4 3 1 1 1	58200408	58195872
10 4 2 2 1 1	25866888	25864872
9 7 4 0 0 0	38802624	38794896
9 6 5 0 0 0	77598528	77596512
8 7 5 0 0 0	116400480	116392080
8 6 6 0 0 0	174608112	174588288
9 7 3 1 0 0	77370	76600
9 6 4 1 0 0	154180	153760
8 7 4 1 0 0	231550	230360
8 6 5 1 0 0	693500	692170
9 7 2 2 0 0	1385880	1385460
9 6 3 2 0 0	462820	461000
8 7 3 2 0 0	1848420	1846740
8 6 4 2 0 0	2773160	2769520
8 6 3 3 0 0	5543520	5541840
9 7 2 1 1 0	11085360	11085360
9 6 3 1 1 0	647706	645606
8 7 3 1 1 0	3234580	3231920
8 6 4 1 1 0	6468850	6464090
9 6 2 2 1 0	12933780	12932100
8 7 2 2 1 0	19402040	19396720
8 6 3 2 1 0	38799600	38797920
8 6 2 2 2 0	3881136	3878616
9 6 2 1 1 1	9702840	9696540
8 7 2 1 1 1	19400640	19398120
8 6 3 1 1 1	12935460	12930420
8 6 2 2 1 1	38801280	38796240
9 5 5 1 0 0	77597520	77597520

9 5 4 2 0 0	58204440	58191840
8 5 5 2 0 0	116398800	116393760
9 4 4 3 0 0	16169760	16162620
8 5 4 3 0 0	48502440	48494460
8 4 4 4 0 0	96998160	96995640
9 5 4 1 1 0	64667160	64662120
8 5 5 1 1 0	97004040	96989760
9 4 4 2 1 0	193996320	193991280
8 5 4 2 1 0	290998680	290982720
8 4 4 3 1 0	129334260	129324180
8 4 4 2 2 0	258658440	258658440
9 4 4 1 1 1	387992640	387982560
8 5 4 1 1 1	581995680	581967120
8 4 4 2 1 1	521000	519040
7 7 6 0 0 0	2079380	2077630
7 7 5 1 0 0	3120540	3116550
7 6 6 1 0 0	6236460	6234570
7 7 4 2 0 0	12471240	12470820
7 6 5 2 0 0	832592	830212
6 6 6 2 0 0	4158480	4155540
7 6 4 3 0 0	8316680	8311360
6 6 5 3 0 0	16628880	16627200
6 6 4 4 0 0	24945000	24939120
7 7 4 1 1 0	49884960	49883280
7 6 5 1 1 0	971840	969178
6 6 6 1 1 0	5821424	5818204
7 6 4 2 1 0	14555240	14546980
6 6 5 2 1 0	29100960	29097180
6 6 4 3 1 0	19402630	19396190
6 6 4 2 2 0	58201640	58194640
7 6 4 1 1 1	116397120	116395440
6 6 5 1 1 1	87308760	87291960
6 6 4 2 1 1	174598200	174590640
11 3 3 3 0 0	17463432	17455452
11 3 3 2 1 0	34920144	34917624
10 3 3 3 1 0	29103480	29094660
11 3 2 2 2 0	87302040	87292380
10 3 3 2 2 0	174595680	174593160
11 3 2 2 1 1	116398800	116393760
10 3 3 2 1 1	174603240	174585600
11 2 2 2 2 1	349191360	349186320
10 3 2 2 2 1	523792920	523773600



10 2 2 2 2 2	36382500	36369900
9 5 3 3 0 0	145500600	145490100
9 5 3 2 1 0	218260560	218234940
9 4 3 3 1 0	436491720	436480380
8 5 3 3 1 0	291000360	290981040
9 5 2 2 2 0	581983920	581978880
9 4 3 2 2 0	872982600	872961600
8 5 3 2 2 0	1309493640	1309441560
8 4 3 3 2 0	387992700	387982620
9 5 2 2 1 1	1163967840	1163957760
9 4 3 2 1 1	1745963520	1745924880
8 5 3 2 1 1	1109966	1107166
8 4 3 3 1 1	6652896	6649536
9 4 2 2 2 1	16632240	16623840
8 5 2 2 2 1	33257760	33254400
8 4 3 2 2 1	22174140	22167420
8 4 2 2 2 2	66515520	66508800
7 7 3 3 0 0	133024320	133024320
7 7 3 2 1 0	99776640	99759840
7 6 3 3 1 0	199539840	199533120
7 7 2 2 2 0	7761742	7757822
7 6 3 2 2 0	23284016	23274496
6 6 3 3 2 0	46560192	46556832
7 7 2 2 1 1	38804140	38793500
7 6 3 2 1 1	116402160	116390400
6 6 3 3 1 1	232794240	232790880
7 6 2 2 2 1	155198460	155191740
6 6 3 2 2 1	232803200	232781920
6 6 2 2 2 2	465588480	465581760
7 5 5 3 0 0	698389440	698365920
7 5 4 4 0 0	46563552	46553472
6 5 5 4 0 0	139680576	139670496
7 5 5 2 1 0	279351072	279351072
7 5 4 3 1 0	58205280	58191000
6 5 5 3 1 0	232797600	232787520
7 4 4 4 1 0	349203120	349174560
6 5 4 4 1 0	698382720	698372640
7 5 4 2 2 0	465595200	465575040
6 5 5 2 2 0	931170240	931170240
7 4 4 3 2 0	1396765440	1396745280
6 5 4 3 2 0	2095161600	2095104480
6 4 4 4 2 0	290999520	290981880

6 4 4 3 3 0	581997360	581965440
7 5 4 2 1 1	1163967840	1163957760
6 5 5 2 1 1	1745961840	1745926560
7 4 4 3 1 1	775985400	775965240
6 5 4 3 1 1	2327935680	2327915520
6 4 4 4 1 1	3491920320	3491856480
7 4 4 2 2 1	3103900920	3103900920
6 5 4 2 2 1	4655871360	4655831040
6 4 4 3 2 1	27166848	27155646
6 4 4 2 2 2	54320814	54315774
5 5 5 5 0 0	54324174	54312414
5 5 5 4 1 0	162961232	162948352
5 5 4 4 2 0	325911264	325907904
5 4 4 4 3 0	67909580	67892500
4 4 4 4 4 0	271598380	271584380
5 5 4 4 1 1	407410640	407375920
5 4 4 4 2 1	814781520	814766400
4 4 4 4 3 1	543195550	543169790
4 4 4 4 2 2	1086368700	1086361980
9 3 3 3 2 0	1629561920	1629533920
8 3 3 3 3 0	2444369760	2444299200
9 3 3 2 2 1	81485376	81469416
8 3 3 3 2 1	325914624	325904544
9 3 2 2 2 2	488880336	488848416
8 3 3 2 2 2	977733792	977723712
7 5 3 3 2 0	407396640	407377320
7 4 3 3 3 0	814791600	814756320
6 5 3 3 3 0	1629552960	1629542880
7 5 3 2 2 1	2444341200	2444302560
7 4 3 3 2 1	1086375420	1086355260
6 5 3 3 2 1	3259105920	3259085760
6 4 3 3 3 1	4888679040	4888608480
7 5 2 2 2 2	1018503360	1018450440
7 4 3 2 2 2	2036946240	2036923560
6 5 3 2 2 2	1357976040	1357937400
6 4 3 3 2 2	4073890800	4073848800
5 5 5 3 2 0	6110877360	6110769840
5 5 4 3 3 0	5431836600	5431816440
5 5 5 2 2 1	8147778240	8147700960
5 5 4 3 2 1	10863673020	10863632700
5 4 4 3 3 1	97780440	97765320
5 5 4 2 2 2	488871936	488856816

5 4 4 3 2 2	977743872	977713632
4 4 4 3 3 2	1955457504	1955457504
7 3 3 3 2 2	2933201376	2933171136
6 3 3 3 3 2	1222184880	1222137000
5 5 3 3 2 2	2444329440	2444314320
5 4 3 3 3 2	1629563040	1629532800
4 4 3 3 3 3	4888658880	4888628640
4 4 4 4 2 2	7333013520	7332917760
5 5 3 3 3 1	6518191680	6518191680
5 5 3 3 2 2	9777317760	9777257280
5 4 4 4 3 0	2036961360	2036908440
5 4 4 4 2 1	6110833680	6110775720
5 4 4 3 3 1	8147754720	8147724480
5 4 4 3 2 2	12221662320	12221556480
5 4 3 3 3 2	16295509440	16295448960
5 3 3 3 3 3	21727305720	21727305720
4 4 4 4 4 0	2546223120	2546142480
4 4 4 4 3 1	10184706000	10184643000
4 4 4 4 2 2	15277122000	15276958200
4 4 4 3 3 2	20369406960	20369291040
4 4 3 3 3 3	27159162480	27159102000

<sup>a</sup>number of hexagonal face colors:  $N(A_g)+N(A_u)$ ; <sup>a</sup>number of chiral pairs of hexagonal face colors:  $N(A_u)$  <sup>a</sup>number of achiral hexagonal face colors:  $N(A_g)-N(A_u)$ .

4. Applications: Chirality, Zeolites, mesoporous, nanomaterials and Biological Networks

Combinatorial enumerations under symmetry action have several applications to chirality, materials and biological networks. In the context of chirality, as shown in the previous section the combinatorial numbers for the totally symmetric  $A_g$  representation for any given color partition enumerates the Pólya equivalence classes of face colorings under the full  $O_h$  or  $I_h$  group. The combinatorial numbers for the chiral  $A_u$  IR yield the number of chiral pairs of face colorings while the difference between  $A_g$  and  $A_u$  numbers yields the number of achiral face colorings. Consequently, the sum of  $A_g$  and  $A_u$  numbers yields the total number of equivalence classes under the pure rotational operations or in  $O$  or  $I$  groups, respectively. As it is well known, chirality arises in a face coloring of the geometrical shapes considered here if the mirror image of the face coloring is not superimposable on the original coloring.

Another interesting application of the combinatorial enumeration scheme considered here is to spectroscopy in the context of nuclear spin statistics under symmetry [17,18,57,58]. In this context, the alternating irreducible representation, which is defined with +1 character values for even permutations and -1 for the odd permutations, plays a critical role in the case of fermion statistics. Consequently, the alternating representation is critical to the quantum chemical classification of the rovibronic wavefunctions of fermions, as the total wavefunction for fermions must be antisymmetric as stipulated by the Pauli Principle. Consequently, the direct product of the nuclear spin functions of the rovibronic and the IR of the rovibronic level of water clusters in the total nonrigid limit would have to transform according to the alternating representation of the hypercube. Consequently, the combinatorial enumerations considered here are extremely useful in the analysis of experimental spectroscopic properties of a number of weakly-bound *van der waals* clusters such as  $(H_2O)_n$ ,  $(NH_3)_n$  and so forth [17,18].

A number of mesoporous materials and zeolite structures are networks of various shapes that we have considered in this study. For example, the structure of the tetragonal zeolite farneseite [64] shown in Figure 4, consists of several truncated octahedra. The combinatorics of a truncated octahedron was considered in Table 4 among several other structures of octahedral or cubic symmetries. Consequently, when dice enumerations are specialized to the case of a few chosen types of colors, the combinatorics considered reduces to face colorings of complex zeolite types of structures like the one shown in Figure 4. That is, face colorings would correspond to the enumeration of isomeric structures that would arise from face capping of zeolite structures, analogous to the one shown in Figure 4. It is hoped that the present work will stimulate such applications to novel nanomaterials in the future.

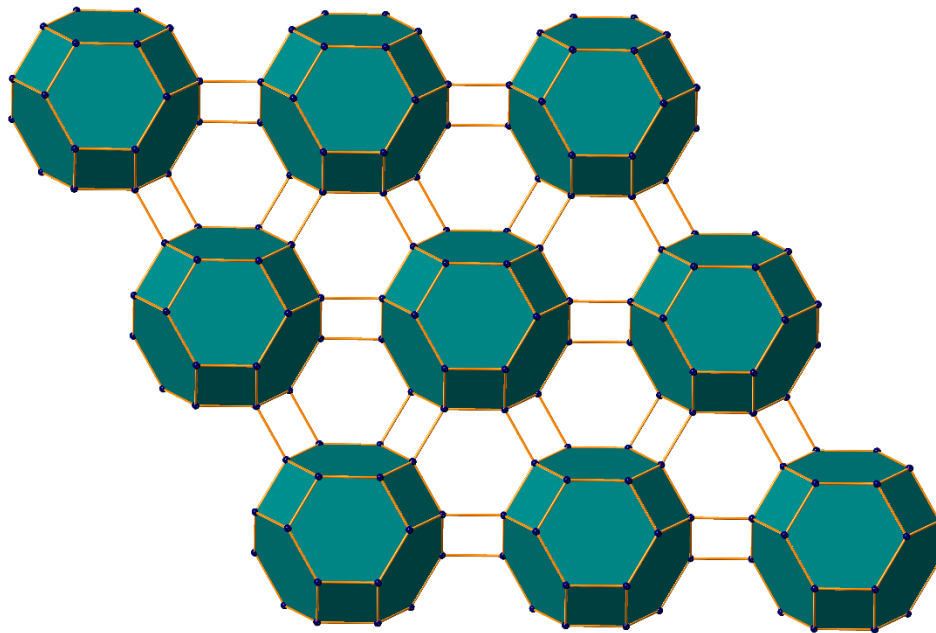


**Figure 4.** The structure of the tetragonal zeolite farneseite comprising of several truncated octahedral. Figure reproduced with permission of authors [64]. The enumeration of structures obtained from face capping of such zeolites correspond to face color enumerations considered in the current study.

Cayley trees are recursive symmetry structures which find a number of applications in biological networks such as phylogenetic trees [51]. The symmetry groups of such structures are recursive wreath products and thus the colorings of vertices or edges of phylogenetic trees follow applications of the techniques considered in this study. These trees also find applications in pandemic trees as demonstrated in recent study on COVID-19 [52]. Moreover, in genetics the canalization or control of one genetic trait by another trait in the genetic regulatory networks is well described by the coloring of vertices of the hypercubes. Such genetic regulatory networks play important roles in evolutionary processes [53,54]. In this context, partitioning 2-colorings of the vertices of hypercubes into equivalence classes yield smaller clustering subsets for the statistical analysis of such networks. Consequently, the properties of any representative in an equivalence class contain the same genetic expression as any other function in the same equivalence class. The hypercubes have applications to the representations of DNA bases including DNA unnatural pairs [6].

## 5. Applications to Cryptography.

The combinatorial complexity of various shapes of dice considered here facilitates their applications to cryptography due to the enormous number of configurations rising from the face colorings and number of chiral dice generated from various shapes. As seen from previous Tables, the numbers grow in astronomical proportions culminating into  $4.4102702121446021496460288562760144 \times 10^{3171}$  for the grand cell-600 dice. Such large combinatorial

numbers relate to the combinatorial complexity of these shapes. Combinatorial complexity can be measured by the number of dice generated for each shape, as this could be one powerful measure of the complexity. The greater is this number the more complex is the structure. The large combinatorial complexity paves the way for powerful applications in cryptography for encrypting and decrypting messages through labeling the faces of the shapes with words or alphabets contained in a message. Once a mapping of the alphabets or other coded parts of a message are mapped to the faces of the shape considered here then the various permutations of the faces would result in enormous number of configurations allowing to scramble the codes message completely.

The Rubik's cube in an excellent exemplification of the underlying combinatorial complexity and thus a great candidate for the puzzle that it is eminent for. As seen from the previous section on Rubik's cube, there are  $5.34018574959804633194496 \times 10^{29}$  possible dice suggesting astronomical number of ways to label the faces of the Rubik's cube. This would indeed enable encryption of messages by labeling the faces of the cube with alphabets or codes. Then the various rotations of the larger faces would scramble the message completely and there are  $5.34018574959804633194496 \times 10^{29}$  such possibilities in the most general case. Consider two romantic clandestine messages to illustrate the point using the Rubik's cube namely, "I Love U" and "V Elope at 2". The first message has 6 alphabets and 2 blank spaces. For example, if say a corner or edge square of each larger face of the Rubik's cube is chosen to label with 6 alphabets in the message and the cube is scrambled by the various rotations. The receiver then would have to solve the Rubik's cube puzzle to decrypt the message. The complexity of the encryption can be further enhanced by mapping alphabets to other characters, simplest would be to map the alphabets to 26 numbers or other characters including !, @, #, \$, %, ^, &, \* and so on to make the message totally look like some sort of gibberish. The other message "V Elope at 2", contains 12 characters, 2 repeating es, 3 blanks and a number 2. If these characters are intertwined with other characters or numbers and one uses say a grand cell-600, one would achieve a bit less than the maximum number of  $4.4102702121446021496460288562760144 \times 10^{3171}$  chiral pairs of configurations. The numbers will be reduced by the repeating 3 blank spaces and two repeating es (assuming upper and lower cases are not differentiated) or by  $3! \times 2!$  provided all other faces are labelled with other unique numbers or characters, we would then arrive at  $3.67522517678717 \times 10^{3170}$  ways to scramble the message "V Elope at 2" using the faces of a grand cell-600 to encrypt the message. Just like the problem of Rubik's cube, the larger encryption puzzles involving n-dimensional objects can be solved by a series of systematic algorithms. The other nuance that can be introduced in n-dimensional encryption algorithms is to use characters to code a message, for example, a simple message: V Elope at 2 becomes ☙ ☞●□□ℳ ☞◆ ☞ in Wingding font. Note that with the increasing importance of artificial intelligence in the coming years, it is very clear that algorithms with machine learning and AI techniques can be developed to decrypt the messages sent through even such complex pockets of objects, for example, a grand cell-600. Indeed n-dimensional hypercubes and other combinatorially complex shapes considered here provide very compelling objects to generate packets of encrypted messages with face or edge or cell or tesseract or other complex p-dimensional hyperplanes for complex encryption that cannot be easily decrypted without invoking very complex AI algorithms that can unravel puzzles in n-dimensional spaces. Consequently, the present investigation on combinatorics of dice of various shapes in n dimensions indeed opens up such a plethora of applications in cryptography with potentials for defense and other applications.

## 6. Conclusions

In the preset study we considered several geometrical forms of dice with octahedral, icosahedral and higher symmetries including the hyperoctahedral symmetries. Combinatorial enumeration of dice for these various shapes as well as the enumeration of dice in n-dimensions were considered. The results not only revealed substantial combinatorial complexities for higher order dice but also the existence of intriguing isochiral dice for some of the geometrical shapes. A number of applications to material science, biology, molecular clusters and cryptography were pointed out. It is clear that

these n-dimensional and other complex objects considered here hold considerable promise as candidates for numerous applications going into the future.

**Author Contributions:**

**Funding:**

**Conflicts of Interest:**

## References

1. Balasubramanian, K. Recursive Symmetries: Chemically Induced Combinatorics of Colorings of Hyperplanes of an 8-Cube for All Irreducible Representations. *Symmetry* **2023**, *15*, 1031. <https://doi.org/10.3390/sym15051031>.
2. Balasubramanian K. Topological Indices, Graph Spectra, Entropies, Laplacians, and Matching Polynomials of n-Dimensional Hypercubes. *Symmetry*. **2023**; *15*(2):557. <https://doi.org/10.3390/sym15020557>
3. Balasubramanian, K. Symmetry, Combinatorics, Artificial Intelligence, Music and Spectroscopy. *Symmetry* **2021**, *13*, 1850. <https://doi.org/10.3390/sym13101850>
4. Carbó-Dorca, R. Boolean hypercubes and the Structure of Vector Spaces, *J. Math. Sci. & Model.* **2018**, *1*, 1-14.
5. Carbó-Dorca, R. N-Dimensional Boolean hypercubes and the Goldbach conjecture, *J Math Chem.* **2016**, *54*, 1213 -1220 <https://doi.org/10.1007/s10910-016-0628-5>
6. Carbó-Dorca, R. DNA unnatural base pairs and hypercubes, *J Math Chem.* **2018**, *56*, 1353-1536. <https://doi.org/10.1007/s10910-018-0866-9>
7. Carbó-Dorca, R.; Chakraborty, T. Quantum similarity description of a unique classical and quantum QSPR algorithm in molecular spaces: the connection with Boolean hypercubes, algorithmic intelligence, and Gödel's incompleteness theorems. In *Chemical Reactivity* **2023**, (pp. 505-572), Elsevier.
8. Carbó-Dorca, R. Boolean Hypercubes as time representation holders, *J Math Chem.* **55**(2018) 1349-1352. <https://doi.org/10.1007/s10910-018-0865-X>
9. Carbó-Dorca, R.; Chakraborty, T. Divagations about the periodic table: Boolean hypercube and quantum similarity connections. *J. Comput. Chem.* **2019**, *40*(30), 2653-2663.
10. Kaatz, F.H.; Bultheel, A. Dimensionality of hypercube clusters. *J. Math Chem.* **2016**, *54*, 33-43.
11. Gowen, A. A.; O'Donnella, C. P.; Cullen, P. J.; Bell, S. J. Recent applications of chemical imaging to pharmaceutical process monitoring and quality control. *European J. Pharmaceutics and Biopharmaceutics*, **2008**, *69*, 10-22.
12. Mezey, P. G. Similarity Analysis in two and three dimensions using lattice animals and polytopes, *J. Math. Chem.* **1992**, *11*, 27-45.
13. Fralov, A.; Jako, E.; Mezey, P. G. Logical Models for Molecular Shapes and Families, *J Math Chem.* **2001**, *30*, 389-409.
14. Mezey, P. G. Some Dimension Problems in Molecular Databases, *J. Math. Chem.* **2009**, *45*, 1.
15. Mezey, P. G. Shape Similarity measures for Molecular Bodies: A Three-dimensional Topological Approach in Quantitative Shape-activity Relation, *J. Chem. Inf. Comput. Sci.* **1992**, *32*, 650.
16. Balasubramanian, K. Combinatorial Multinomial Generators for colorings of 4D-hypercubes and their applications, *J. Math. Chem.* **2018**, *56*, 2707-2723.
17. Balasubramanian, K. Nonrigid group theory, tunneling splittings, and nuclear spin statistics of water pentamer: (H<sub>2</sub>O)<sub>5</sub>. *J. Phys. Chem. A* **2004**, *108*, 5527-5536.
18. Balasubramanian, K. Group-Theory and Nuclear-Spin Statistics of Weakly-Bound (H<sub>2</sub>O)<sub>N</sub>, (NH<sub>3</sub>)<sub>N</sub>, (CH<sub>4</sub>)<sub>N</sub>, and NH<sub>4</sub><sup>+</sup>(NH<sub>3</sub>)<sub>N</sub>. *J. Chem. Phys.* **1991**, *95*, 8273-8286.
19. Clifford, W. K. On the types of compound statement involving four classes, *Proc Manchester Literary and Philosophical Soc.*, **1877**, 88-101.
20. Clifford, W. K., Mathematical Papers. Editor: R. Tucker, R. McMillan & Co, London, 1882, Introduction by H. J. Stephen Smith, Reprinted by Chelsea, NY 1968.
21. M. A. Harrison and R.G. High, On the cycle index of a product of permutation group, *J. Combin. Theory* **4** (1968), 277-299.
22. Pólya, G.; Read, R. C. *Combinatorial Enumeration of Groups, Graphs and Chemical Compounds*, Springer, New York **1987**.
23. Pólya, G. Sur les types des propositions composées, *J. Symbolic Logic* **1940**, *5*, 98-103.



24. Banks, D. C.; Linton, S. A.; Stockmeyer, P. K. Counting Cases in Substotope Algorithms, *IEEE Trans. Visualization & Computer Graphics*, **2004**, 371-384.
25. Bhaniramka, P.; Wenger, R.; Crawfis, R. Isosurfacing in higher Dimension. *Proc. of IEEE Visualization* **2000**, pp.267-270.
26. Aichholzer, O. Extremal Properties of 0/1-Polytopes of Dimension 5. Polytopes - Combinatorics and Computation, . Editors: Ziegler, G. & Kalai, G. Birkhäuser, **2000**, pp.11-130.
27. Perez-Aguila, R. Enumerating the Configurations in the n-Dimensional Polytopes through Pólya's counting and A Concise Representation, in, **2006**, Third International Conference on Electrical and Electronics Engineering, pp1-4, IEEE.
28. Banks, D. C.; Stockmeyer, P. K. De Bruijn Counting for visualization Algorithms, Math Found. Sci. Visualization, computer graphics and Massive data exploration, Springer, Berlin **2009**, pp 69-88.
29. Perez-Aguila, R. Towards a New Approach for volume datasets based on orthogonal polytopes in four-dimensional color space, *Engineering Letters* **2010**, 18:4,326, EL\_18\_4\_02
30. Chen, W. Y. C.; Guo, P. L. Equivalence Classes of Full-Dimensional 0/1-Polytopes with Many Vertices, Jan **2011**, <https://arxiv.org/pdf/1101.0410.pdf>
31. Chen, W. Y. C. Induced cycle structures of the hyperoctahedral group, *SIAM J. Disc. Math.* **1993**, 6, 353-362.
32. Ziegler, G. M. Lectures on Polytopes. *Graduate Texts in Mathematics*, 52, Springer-Verlag, **1994**.
33. Lemmis, P. W. H. Pólya Theory of hypercubes *Geometriae Dedicata* **1997**, 64,145-15
34. Harary, F.; Palmer, E. M. Graphical Enumeration (Academic press, New York, NY, 1973).
35. Liu, M.; Bassler, K. E. Finite size effects and symmetry breaking in the evolution of networks of competing Boolean nodes. *J. Phys. A: Mathematical and Theoretical* **2010**, 44, 045101.
36. Reichhardt, C. J. O; Bassler, K. E. Canalization and symmetry in Boolean models for genetic regulatory networks. *J. Phys. A: Mathematical and Theoretical* **40** (2007) 4339.
37. Balasubramanian, K. Applications of Combinatorics and Graph Theory to Quantum Chemistry and Spectroscopy, *Chem. Rev.* **1985**, 85,599-618.
38. Balasubramanian, K. Symmetry Groups of Nonrigid Molecules as Generalized Wreath-Products and Their Representations, *J. Chem. Phys.* **1980**, 72, 665-677.
39. Balasubramanian, K Nonrigid water octamer: Computations with the 8-cube. *J. Comput Chem.* **2020**, 41, 2469- 2484.
40. Balasubramanian, K. Computations of Colorings 7D-Hypercube's Hyperplanes for All Irreducible Representations. *J. Comput Chem.* **2020**, 41, 653-686.
41. Balasubramanian, K. Relativistic double group spinor representations of nonrigid molecules. *J. Chem. Phys.* **2004**, 120,5524-5535.
42. Balasubramanian, K. Generalization of De Bruijn's Extension of Pólya's Theorem to all characters, *J. Math. Chem.* **1993**, 14,113-120.
43. Balasubramanian, K. Generalization of the Harary-Palmer Power Group Theorem to all Irreducible Representations, *J. Math. Chem.* **2014**,52,703-728.
44. Balasubramanian, K., Enumeration of Internal-Rotation Reactions and Their Reaction Graphs. *Theor. Chim. Acta.* **1979**, 53, (2), 129-146.
45. Wallace, R. Spontaneous symmetry breaking in a non-rigid molecule approach to intrinsically disordered proteins. *Molecular BioSystems*, **2012**, 8(1), 374-377.
46. Wallace, R. Tools for the Future: Hidden Symmetries. In *Computational Psychiatry* **2017**, (pp. 153-165). Springer, Cham.
47. Darafsheh, M. R. ; Farjami, Y.; Ashrafi, A. R. Computing the Full Non-Rigid Group of Tetranitrocubane and Octanitrocubane Using Wreath Product. *MATCH Commun. Math. Comput. Chem* **2005**, 54,53.
48. Foote, R.; Mirchandani, G.; Rockmore, D. A two-dimensional Wreath Product Transforms. *J. Symbolic Computation* **2004**, 37, 187-207.
49. Balasubramanian, K. A Generalized Wreath Product Method for the Enumeration of Stereo and Position Isomers of Polysubstituted Organic Compounds. *Theor. Chim. Acta.* **1979**,51, 37 -51.
50. Balasubramanian, K. Symmetry Simplifications of Space Types in Configuration-Interaction Induced by Orbital Degeneracy, *Int. J. Quantum Chem.* **1981**, 20,1255-1271.
51. Balasubramanian, K.Nested wreath groups and their applications to phylogeny in biology and Cayley trees in chemistry and physics. *J. Math. Chem.* **2017**, 55, 195-222.

52. Nandini, G.K.; Rajan, R.S.; Shantrinal, A.A.; Rajalaxmi, T.M.; Rajasingh, I.; Balasubramanian, K. Topological and Thermodynamic Entropy Measures for COVID-19 Pandemic through Graph Theory. *Symmetry* **2020**, *12*, 1992. <https://doi.org/10.3390/sym12121992>
53. Rousseau, R. On Certain Subgroups of a Wreath Product", *Match*. **1982**, *13*, 3-6.
54. Florek, W.; Lulek, T.; Mucha, M. Hyperoctahedral groups, wreath products, and a general Weyl's recipe. *Zeitschrift für Kristallographie-Crystalline Materials*, **1988**, *184*, 31-48.
55. Balasubramanian, K. Generators of the Character Tables of Generalized Wreath Product Groups. *Theor. Chim. Acta.* . **1990**, *78*,31-43.
56. Liu, X. Y.; Balasubramanian, K. Computer Generation of Character Tables of Generalized Wreath Product Groups *J. Comput. Chem.* **1990**, *11*, 589-602.
57. Balasubramanian, K. A Method for Nuclear-Spin Statistics in Molecular Spectroscopy. *J. Chem. Phys.* **1981**, *74*,6824-6829.
58. Balasubramanian, K. Operator and algebraic methods for NMR spectroscopy. I. Generation of NMR spin species. *J. Chem. Phys.* **1983**, *78*, 6358-6368.
59. Coxeter, H. S. M. Regular Polytopes, Dover Publications, New York, **1973**.
60. T. Ruen, By self - Own work, free public domain work available to anyone to use for any purpose. <https://commons.wikimedia.org/w/index.php?curid=11743942>
61. Bandelow, C. *Inside Rubik's cube and beyond*. **2012**, Springer Science & Business Media.
62. User: Imk3nnyma, CC BY-SA 4.0, <https://commons.wikimedia.org/w/index.php?curid=79057596>
63. Buck, D. K.; Collins, A. A., POV-RAY, <https://en.wikipedia.org/wiki/User:Cyp/Poly.pov> <https://en.wikipedia.org/wiki/User:Cyp/Poly.pov>Public Domain, CC BY-SA 3.0
64. Jacob,K.; Clement,J.; Micheal Arockiaraj,M.; Peter, P.; Balasubramanian, K. Distance-based topology and entropy analysis of tetragonal farneseite zeolites, Submitted for Publication, **2024**.
65. Balasubramanian, K. Double group of the icosahedral group (Ih) and its application to fullerenes. *Chem. Phys. Lett.* **1996**, *260*, (3-4), 476-484.
66. Kroto, H. W., Heath, J. R.; O'Brien, S. C.; Curl, R. F.; Smalley, R. E. C<sub>60</sub>:Buckminsterfullerene. *Nature* **1985**, *318*, 162-163.
67. Kroto, H. W., Heath, J. R.; O'Brien, S. C.; Curl, R. F.; Smalley, R. E. Long Carbon Chain Molecules in Circumstellar Shells, *Astrophys. J.* **1987**, *314*, 352-355.
68. Balasubramanian, K.; Liu, X. Y. Spectra and Characteristic Polynomials of Polyhedral Clusters. *Int. J. Quantum Chem.* **1988**, *22*, (S), 319-328.

**Disclaimer/Publisher's Note:** The statements, opinions and data contained in all publications are solely those of the individual author(s) and contributor(s) and not of MDPI and/or the editor(s). MDPI and/or the editor(s) disclaim responsibility for any injury to people or property resulting from any ideas, methods, instructions or products referred to in the content.